National Physical Laboratory

NPL REPORT IR 29

The NPL contribution to CCRI key comparison K8 of thermal neutron fluence measurements

P K Kolkowski and D J Thomas

JULY 2013

National Measurement System

July 2013

NATIONAL PHYSICAL LABORATORY

The NPL contribution to CCRI key comparison K8 of thermal neutron fluence measurements

by

P. Kolkowski and D.J. Thomas

Neutron Metrology Group
Acoustics & Ionising Radiation Division

Abstract
The results of NPL's experiments as part of the CCRI key comparison, K8, of thermal neutron fluence measurements are presented. Two detectors were provided for the comparison, and measurements were performed for both detectors, with and without the polyethylene moderating sphere provided. These measurements were performed with the detectors orientated both parallel and perpendicular to the neutron beam from the column of the NPL thermal pile.

ISSN 1754-2952

National Physical Laboratory
Hampton Road, Teddington, Middlesex, TW11 0LW

This report details the results of NPL's participation in a CCRI key comparison of thermal neutron fluence production and measurement. A restricted report was originally produced, printed as NPL REPORT AIR(RES)024, and was sent to the evaluator. The results of the comparison have now been made public so this report has been re designated as IR 29 and published as a NOT RESTRICTED report.

Approved on behalf of the Managing Director, NPL by Bajram Zeqiri,
Knowledge Leader, Acoustics & Ionising Radiation Team,

Contents

Figures **Page**

Tables **Page**

1 INTRODUCTION

This report details the NPL contribution to CCRI key comparison, K8, of thermal neutron calibration capabilities. There is no standard technique that is used by national metrology institutes (NMIs) for producing thermal neutron calibration fields. They can be reactor-based systems, or can be based on a neutron source, or sources, in a moderating assembly. The neutron source can be either a radionuclide source, or on accelerator-driven one. Probably because of the diversity of the facilities, this is the first CCRI thermal neutron comparison to have been organised.

The comparison involved circulating two SP9 spherical ^{3}He proportional counters as thermal neutron detectors – see the protocol at Appendix A. These have response functions which decrease with a roughly $1/v$ dependence on energy over the thermal region, where v is the neutron velocity. They differed in gas pressure and hence sensitivity; one, serial no. 8916-104, contained 200 kPa of the gas and the other, serial no. 9313-111, only 20 kPa. This allowed measurements to be made over a wide range of different neutron fluence rates, up to roughly 10^5 cm^{-2} s^{-1}, although this range does not extend to the fluences typically found in, or close to, the core of a reactor. In addition a 7.62 cm (3") diameter polyethylene moderating sphere was made available. Either of the SP9 counters could be positioned at the centre of this sphere to provide a neutron detector with a very different response function for thermal neutrons, in fact one that increases with energy over the thermal region. The motivation for using of this combination of instruments was to obtain information on the neutron spectra at the various participating laboratories. Basically, the ratio of the responses of the bare and moderated instruments gives an indication of the mean energy of the thermal distribution.

The detectors were circulated to the participating labs together with a set of battery-operated electronics and the protocol. This explained how to use the equipment, and also detailed the quantity to be reported. This quantity is simply the response of the devices in terms of counts per unit fluence; however, the results need to be corrected to the response which would be obtained in a particular thermal neutron distribution. This approach was necessary so that results from the various laboratories with different thermal neutron fields could be compared.

Thermal neutron fluences are commonly measured using thin activation foils. These are usually irradiated both bare and under a thermal neutron absorbing cadmium cover to derive information about the ratio of the neutron fluence rate above and below the cadmium cut-off energy, which is about 0.5 eV for 1 mm of cadmium. This is the approach adopted at NPL and the foils used are 0.05 mm thick gold. Without detailed information about the thermal neutron spectrum, obtained for example using a mechanical chopper device, the interpretation of activation measurements involves making various assumptions about the spectrometric and directional characteristics of the field.

Thermal fluences derived from activation measurements are normally quoted using the convention of Westcott *et al.*[(1)]. This assumes that the neutron spectrum can be described in terms of a thermal Maxwellian peak and a $1/E$ slowing down component, and the approach is applicable when using foils of materials such as gold which have a cross section which essentially varies inversely as the neutron velocity, i.e. “obeys the $1/v$ law”. The directional characteristics need to be known to derive some of the parameters used in the analysis with this convention. Fluence distributions tend to be either isotropic or approximate to beam geometry. For the present measurements the thermal neutron field was essentially a beam.

In the Westcott convention, the quantity derived is the product of a neutron density, n, and a particular velocity, $v_o = 2200 \text{ m s}^{-1}$. This is a measure of the fluence rate, although not a precise one because the velocity v_o is not the correct average velocity of the neutrons. The reason for using the Westcott approach is that the exact spectrum in most thermal neutron fields is not known, but the use of this convention allows measurements, e.g. of cross sections, to be compared without confusion.

When foil irradiations are performed with and without a cadmium cover a number of different Westcott fluence rates can be derived. In order to determine true fluence rates information is needed on the average velocity of the neutrons, and for this a value is required for the effective temperature, T, of the Maxwellian distribution. (The peak energy of the Maxwellian distribution is at kT, where k is the Boltzmann constant.) With this information the true fluence rates can be derived. Information on the estimation of the temperature of the NPL thermal column field is given in section 2.3. (The Maxwellian temperature is in fact required even to derive nv_0, but the result is not very sensitive to the exact value of T.)

In activation foil measurements the thermal fluence rates are derived from the saturated activity induced in the foils, The expressions relating the saturated activity of the bare foil, D_0, and of the cadmium covered foil, $D_0(Cd)$, to the Westcott fluence rates can be found in various references[2,3,4], and are given below for the most commonly used fluence rates.

$$\phi_W = nv_0 = \frac{1}{G_t} \cdot \frac{(D_0 - D_0(Cd).F)}{N\sigma_0 g} \cdot \frac{R}{(R-1)} \tag{1}$$

$$\phi_W(th) = n_{th}v_0 = \frac{1}{G_t} \cdot \frac{(D_0 - D_0(Cd).F)}{N\sigma_0 g} \tag{2}$$

$$\phi_W(M) = n_M v_0 = nv_0 \left[1 - \frac{4r}{(\pi\mu)^{1/2}}\right] \tag{3}$$

$$\phi_W(1/E) = n_{1/E}v_0 = nv_0 - n_M v_0 \tag{4}$$

$$\phi'_W(1/E) = n'_{1/E}\, v_0 = n_{th}v_0 - n_M v_0 \tag{5}$$

Where:

ϕ_W	is the total fluence rate in the Westcott convention,
G_t	is the thermal neutron self-shielding factor, (it depends on the directional characteristics of the field),
N	number of gold atoms per mg of foil,
σ_0	cross section for 2200 m s^{-1} neutrons,
F	is a correction factor for attenuation of epi-cadmium neutrons in cadmium,
g	is a measure of the departure of the cross section from a $1/v$ dependence in the Maxwellian region (it has a slight dependence on the Maxwellian temperature T),

R	is the cadmium ratio for an ideal 1/*v* detector, which can be derived from the cadmium ratio, $R_{Cd} = D_0 / D_0(Cd)$, measured for the activation foil,
$\phi_W(th)$	is the sub-cadmium-cut-off fluence rate, sometimes called simply the thermal fluence, in the Westcott convention,
n_{th}	is the neutron density in the sub-cadmium-cut-off region,
$\phi_W(M)$	is the Maxwellian fluence rate in the Westcott convention,
n_M	is the neutron density in the Maxwellian distribution,
r	is a measure of the relative intensity of the epithermal component, (expressions for *r* can be found in references 2 and 3),
μ	defines the lower limit, E_Δ, of the 1/*E* component, $E_\Delta = \mu kT$,
$\phi_W(1/E)$	is the total 1/*E* neutron fluence rate in the Westcott convention,
$n_{1/E}$	is the total neutron density in the 1/*E* distribution,
$\phi'_W(1/E)$	is the 1/*E* neutron fluence rate, in the Westcott convention, in the region between E_Δ and the cadmium cut-off energy E_{Cd}, and
$n'_{1/E}$	is the neutron density in the 1/*E* distribution in the region between E_Δ and the cadmium cut-off energy E_{Cd}.

If the value for the effective temperature, *T*, of the Maxwellian is known, a value for, $\bar{v}_M$, the mean velocity for the Maxwellian distribution can be derived[(2-4)]:

$$\frac{\bar{v}_M}{v_0} = \left[\frac{4T}{\pi T_0} \right]^{1/2} \tag{6}$$

where:

T_0 is 293.6 K, i.e. the temperature corresponding to the velocity v_0.

The 1/*E* component is assumed to extend from some lower energy limit E_Δ up to the maximum energy in the spectrum. The average velocity $\bar{v}_{1/E}$ can be calculated from:

$$\frac{\bar{v}_{1/E}}{v_0} = \frac{\ln(E_{\max} / E_\Delta)}{2E_0^{1/2}\left[E_\Delta^{-1/2} - E_{max}^{-1/2} \right]} \tag{7}$$

where:

E_{max} is the maximum energy of the 1/*E* component.

If E_{max} is set to the cadmium cut-off energy, E_{Cd}, the value derived for $\bar{v}_{1/E}/v_0$, indicated here by $\bar{v}'_{1/E}/v_0$, is for the 1/*E* fluence below this energy, i.e. in the thermal region. Thus $\bar{v}$ is available for both components of the fluence below this energy, and the true sub-cadmium-cut-off fluence rate $\phi(th)$ can be derived from:

$$\phi(th) = n_{th}\bar{v}_{th} = n_M \bar{v}_M + n'_{1/E}\,\bar{v}'_{1/E} = n_M v_0 \cdot \frac{\bar{v}_M}{v_0} + n'_{1/E}\, v_0 \cdot \frac{\bar{v}'_{1/E}}{v_0} \tag{8}$$

If the SP9 detectors for the comparison exercise are irradiated in the thermal column field both bare and with a cadmium cover, and the thermal neutron count rate is determined by subtracting the under cadmium counts from the bare counts, then the fluence which produced these counts is given by eq. (8) .

2 THE NPL THERMAL NEUTRON FACILITY

2.1 History and construction

Thermal neutron fluence standards have been available at NPL since the facility, commonly known as the thermal pile, was set up in the late 1960s by Ryves and Paul[5]. The pile consists of a large graphite block within which fast neutrons are produced by bombarding two beryllium targets, located on either side of a central irradiation cavity, with deuterons from the NPL 3.5 MV Van de Graaff accelerator. The graphite moderates these neutrons producing a well thermalized field at the bottom of the cavity. Figure 1 shows a schematic view of the pile.

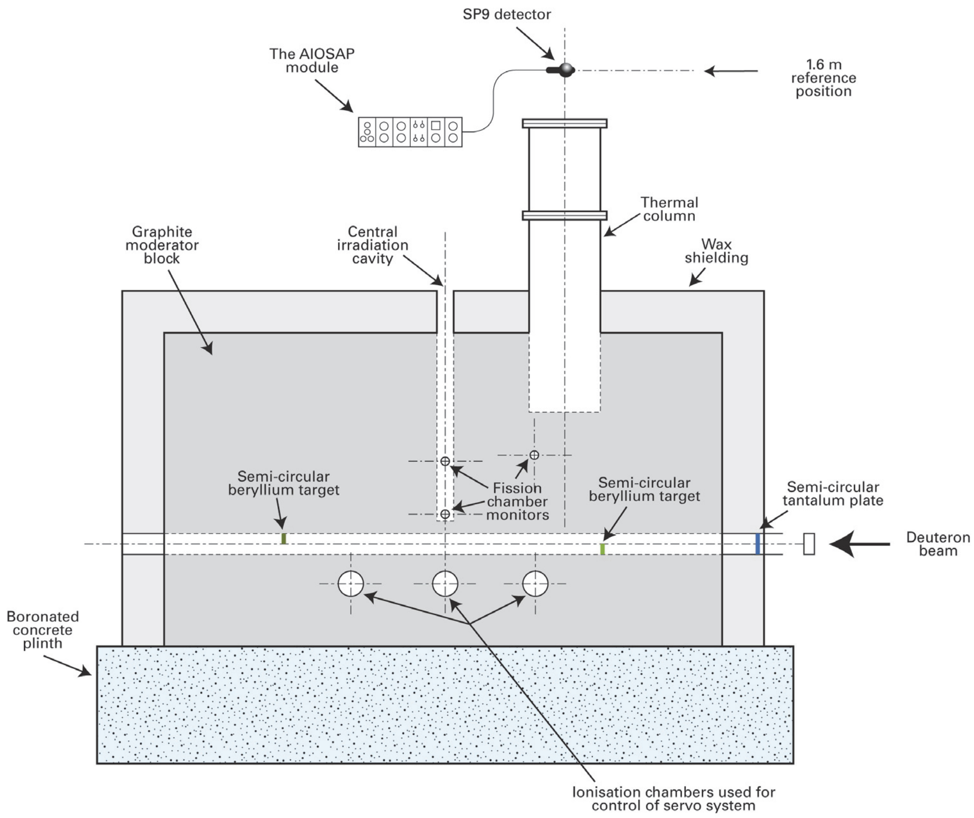

Figure 1. Side-on schematic view of the NPL thermal pile.

The arrangement of the targets as two semi-circular plates, in combination with a semi-circular tantalum ‘dump’ plate just outside the pile, see Figure 2, allows accurate control of the neutron production. The system, described in detail in reference 5, is designed to provide a stable neutron fluence rate at the bottom of the central irradiation cavity, and this fluence rate is controlled by an ionisation chamber situated immediately below the cavity. A servo-system compares the voltage developed by the ion chamber current with a pre-set reference voltage. The fluence rate is then kept constant at a level determined by the reference voltage. Historically this is referred to as the ‘demand level’. Provided the incident deuteron beam intensity remains reasonably constant the servo-system maintains a thermal neutron fluence rate that varies by <± 0.2% over a period of several hours. This is achieved by using steering plates to either move the deuteron beam further onto the tantalum, to reduce the fluence rate, or further onto the beryllium targets, to increase the rate. In this way the system maintains a constant fluence in the cavity regardless of small changes in the total beam current from the Van de Graaff. Two additional ion chambers, situated to the left and right of the central chamber, provide signals to steer the beam vertically between the beryllium targets to keep the yield from the two targets equal and thus minimise the fluence gradient across the floor of the cavity. This cavity is designed for irradiating devices to relatively high neutron fluences, up to 10^7 cm^{-2} s^{-1}. Devices such as SP9 counters are, however, more easily irradiated in the field of the thermal column shown to the left of the cavity in Figure 1.

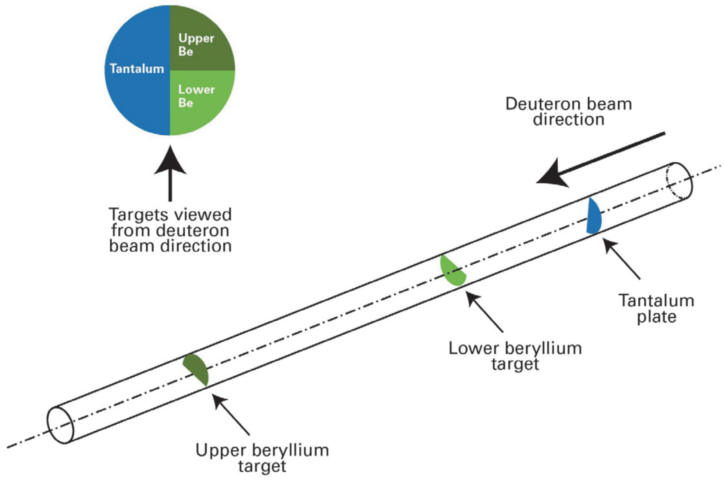

Figure 2. Arrangement of the two beryllium targets and the tantalum plate.

The column consists of a larger diameter hole, also in the top of the pile, but situated so that it is almost over one of the beryllium targets. A stainless steel tube, cadmium-lined on its curved surface, but not on its base, is placed in the hole. The tube is available in sections and can be adjusted in half metre steps, from 1 m to 3 m. When the tube is 1.5 m long or more it can be evacuated to reduce attenuation of the thermal beam. The neutron beam emerging from this tube is reasonably uniform. Over a horizontal circular area of about 10 cm diameter the decrease in fluence from the centre to the extremity of this area is < 1%. For a horizontal circular area of 30 cm diameter the fluence at the extremity is about 6% less than that at the centre. The intensity falls off as the height increases, and the maximum thermal fluence rate achievable at a height of 1 m is about 4 x 10^4 cm^{-2} s^{-1}. Experience has shown that, the control system, although designed to maintain an accurately constant fluence rate at the bottom of the central cavity, also maintains a very constant fluence rate in the beam of the column. The location of the SP9 detectors in the beam of the column during the comparison measurements is shown in Figure 1.

2.2 Monitoring

During the SP9 counter measurements the neutron fluence was continuously monitored by two Centronic, pulsed ^{235}U fission chambers. One is permanently positioned in the graphite between the bottom of the thermal column and the beryllium target (FC_C, type FC4A/100/U235) and the other at a fixed position to one side of the central irradiation cavity (FC_H , type FC4B/20/U235) approximately 60 cm from the axis of the thermal column*.

* Two fission chambers are shown close to the central cavity in Figure 1. FC_H is the upper one of these two.

These monitors were calibrated in terms of the neutron fluence rate at a reference position, 1.6 m above the base of the thermal column, using the gold foil activation technique. The 1.6 m position was chosen so that the required fluence rates could easily be achieved whilst keeping dead time corrections for the SP9 counters reasonably low.

Calibration of the monitors was performed mid-way through the measurements with the SP9 counters. A pair of gold foils, both 1 cm^2 in area and weighing approximately 96 mg, were irradiated, one foil being enclosed in a 1 mm thick cadmium metal box in order to enable the epi-thermal neutron correction to be determined. The foils were mounted on a low mass jig that positioned each foil on a horizontal plane about 4 cm from the central axis of the thermal column at the same height as the SP9 counters were positioned. They were sufficiently far apart that scatter between the foils was negligible.

The foils were 4πβ-counted in shielded, low-background, proportional counters. The observed count rates were corrected for counter background, dead-time, decay during counting, and for non-saturation during the irradiation. The quantity derived for each foil was the saturated β count rate per mg of gold. Foil activities were then derived using β-counting efficiencies determined by 4πβ-γ coincidence counting following irradiation of the foils in the GLEEP reactor at Harwell[2]. The measured β-counting efficiency for the bare gold foils was corrected for the effects of different irradiating spectra at GLEEP and NPL by a correction factor derived from the measured ratios of the activities of the bare and cadmium-covered foils (the cadmium ratios). The counting efficiency of the cadmium-covered foils did not require this correction.

Thermal neutron fluence rates were calculated according to the convention of Westcott *et al.*[1]. A value of (98.69 ± 0.28) barn, taken from the evaluation of Carlson *et al.*[6], was used for the gold activation cross section, σ_0. Appendix B shows the printout of the FORTRAN program which was used to derive the various fluence values from the saturated disintegration rates measured for the bare and cadmium covered foils.

2.3 Spectrum of the thermal column field

Two approaches have been used to derive information about the neutron spectrum in the field of the NPL thermal column. One for the fluence above the cadmium cut off energy, and another for the region below this energy.

The epithermal component of the column spectrum consists of primary neutrons which have not been moderated to thermal energies. These neutrons are produced within the pile from the d-Be reaction, and to a lesser extent, from the d-D reaction and from the action of the deuteron beam on contaminants deposited on the beryllium targets and the tantalum plate. All these reactions contribute to the neutron field, but the ratio of the thermal component to the fast and epithermal component will vary slightly depending on the deuteron beam conditions (energy) and the cleanliness of the vacuum system, targets and tantalum plate. This component has been measured using Bonner spheres. The measurements[7] revealed a relatively flat, 1/E, spectrum extending from the thermal region to a maximum energy of about 8 MeV. Although the higher energy fluence is only about 24% of the thermal fluence, the dose equivalent due to the fast component is more than a factor of two greater than that due to the thermal neutrons.

A second approach was used to derive information about the sub-cadmium part of the spectrum. When analysed using the Westcott convention measurements with gold foils, with and without cadmium cover, provide information on the relative fluences in the Maxwellian peak and in the 1/E component of the spectrum. By using an empirical relationship the effective temperature of the Maxwellian peak can also be determined from these measurements[8]. This approach is described in NPL Report DQL RN008[9], however, since that report was written it has been realised that the effective temperature varies somewhat with height in the column. The most recent measurements give a value of 22.6 °C for T-T_m at the height of 1.6 m where the present measurements were made, where T is the effective temperature of the Maxwellian distribution and T_m is the physical temperature of the moderator. This is measured using a thermometer set inside the pile.

3 MEASUREMENTS

The measurements for the comparison were carried out in the second half of February, 2007.

A battery-powered electronics module was supplied for the measurements, the AIOSAP (All-in-one Spectrometry Processor) which consisted of a high voltage supply, analogue pulse processing, and discrimination units. This module was mounted as close as practical to the thermal neutron beam so that the special cables and sockets supplied could be used to optimise the pulse processing – see Figure 3 lower.

The SP9 counter was connected to the unit with all the settings made as directed in Appendix 1. The high voltage control was slowly increased and then 'locked' when the appropriate value was indicated in the LED display. On several occasions it was noticed that the voltage would slowly increase for about an hour after the initial 'power on' after which it would remain constant at which point the voltage would be reduced to the correct operating value. The increase was as much as 10 volts on one occasion. For this reason the AIOSAP and high voltage were switched on at least two hours prior to the measurements. The discriminator output from the AIOSAP was then connected, via a 30 m 50Ω cable, to an NPL width/delay unit. This unit produces output pulses of a suitable width and height to trigger the scaler card used to record the counts during the measurements. The width of a pulse from this unit is unaffected by the input pulse width and it was set to 6.4 μs for the present measurements.

The electronics for both fission chamber monitors consisted of a high voltage unit, a preamplifier, a main amplifier, a single channel analyser to set a discriminator level above the noise, and a width/delay unit to provide a suitable pulse for counting the events in a scaler. For the column fission chamber short pulse shaping times were used and the dead-time (5.0 ± 0.5 μs) was defined by the width of the pulse from the width/delay unit. For the fission chamber near the central cavity longer pulse shaping times were used in the main amplifier. The pulse from the width/delay unit was set to 10.2 μs, however, subsequent investigation showed that, because of the longer shaping time constants, the overall dead-time per pulse was greater than 10.2 μs and the value used for performing corrections was 11.5 ± 1.0 μs. Before and after any measurements were carried out the ratio of the dead-time corrected fission chamber monitor count rates was compared with previous measurements to check the stability of the monitors.

A locating jig was attached to the top of the thermal column; see Figure 3, which provided a reference plane enabling accurate positioning of the sensitive volume of the bare SP9 counters in all orientations used, and in moderator/cadmium shield assemblies. Sets of pillars of different lengths were used to support the jig so that for every configuration and assembly combination the centre of the sensitive volume was at the reference height of 1.6 m.

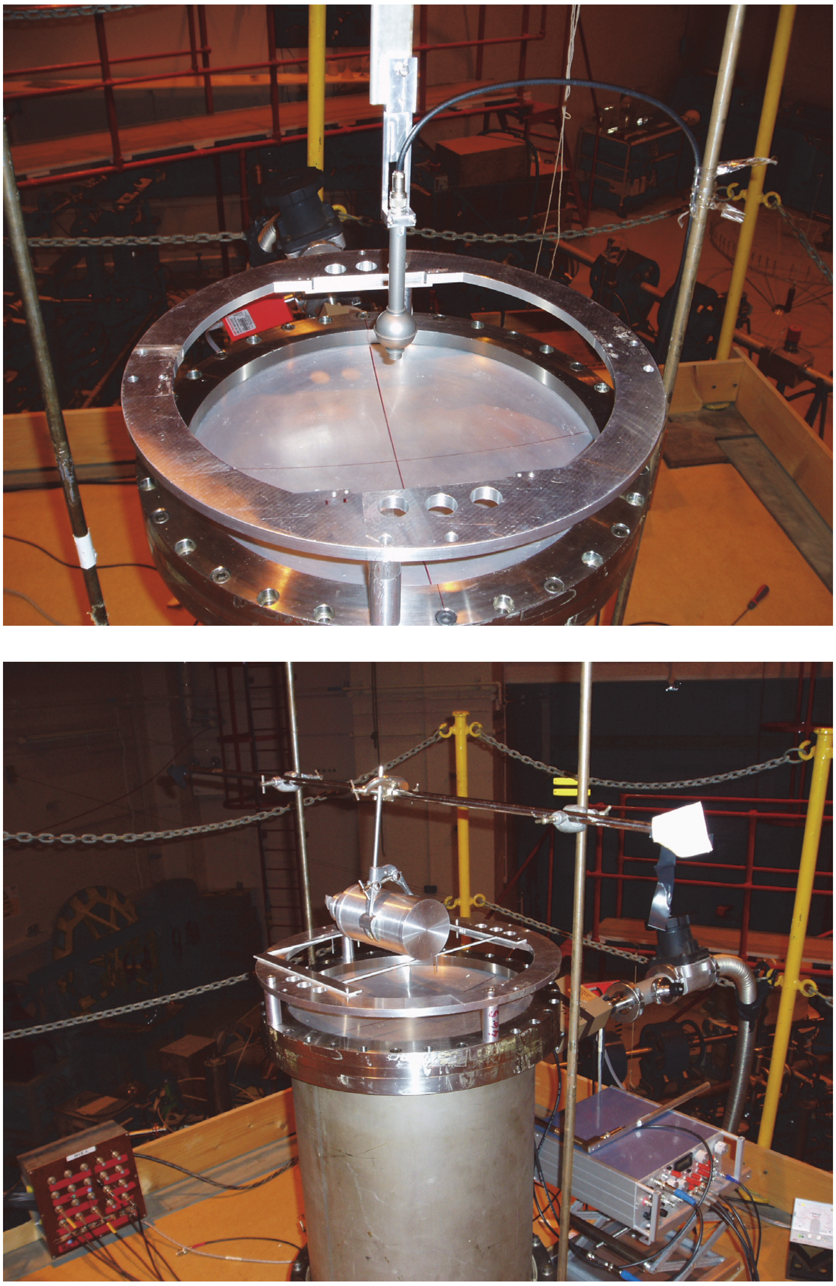

Figure 3. Mounting arrangements for the SP9 counters. Upper picture: SP9 counter bare and parallel to the neutron beam, lower picture SP9 counter in moderator and inside cadmium sleeve mounted perpendicular to the neutron beam.

During all the measurements with the SP9 counter, data were collected via a PC scaler card which recorded: the counts from a precision pulse generator running at 10 Hz, the counts from the SP9 detector, and the counts from the two fission chambers. A measurement consisted of a number of cycles, usually five, each cycle run for 1000 counts from the 10 Hz pulser, i.e. for 100 s. In this way estimates of the statistical uncertainties could be derived from the standard deviation of the cycles as well as from the assumption that Poisson statistics apply. For the measurements with gold foils the counts from the two fission counters were recorded for 100 s cycles throughout the measurement providing information which could be used to correct for any non-uniformity of the irradiation over the period of the measurement.

Table 1 lists the demand levels used for the various measurements performed with the AIOSAP electronics. The levels were chosen to optimise the count rate and in some instances to obtain information about the consistency of the SP9 count rate per unit monitor with demand.

Table 1. Demand levels used for the various measurements with the AIOSAP electronics.

Configuration	Demand level(s)
200 kPa SP9 parallel to the beam no polyethylene moderator	0.1 to 10.0
200 kPa SP9 perpendicular to the beam no polyethylene moderator	0.3
20 kPa SP9 parallel to the beam no polyethylene moderator	0.3 and 3.0
20 kPa SP9 perpendicular to the beam no polyethylene moderator	0.3 and 3.0
200 kPa SP9 parallel to the beam with polyethylene moderator	0.5
200 kPa SP9 perpendicular to the beam with polyethylene moderator	0.5
20 kPa SP9 parallel to the beam with polyethylene moderator	3.0
20 kPa SP9 perpendicular to the beam with polyethylene moderator	3.0

Measurements for all the configurations in Table 1 were performed with and without cadmium cover. For the under-cadmium measurements the SP9 counter was attached to an aluminium base unit and the cover fitted – see Appendix 1. This base unit did not appear to have a cadmium layer, and it was thought that with the SP9 counter perpendicular to the beam there might be a path for thermal neutrons through the base. For this reason an additional cadmium disc was made with a hole at the centre for the SP9 stem and this was fitted on the base unit so that it was on the inside of the final enclosure. However, measurements with and without this disc were consistent within the uncertainties indicating that there was no significant pathway for thermal neutrons through the base.

In addition to collecting data with the AIOSAP electronics some measurements were also performed with conventional NIM electronics units belonging to NPL. The electronics chain consisted of:

- High voltage unit (Tenelec TC953),
- Pre-amplifier (Ortec 142PC),
- Main amplifier (Ortec571),
- Timing Single Channel Analyser (Ortec 551),
- NPL width/delay unit (width of output pulse set to 6.4μs)

The data from these measurements have not been included in the final results for NPL's contribution to this comparison, but have simply been used as a check that results obtained with the AIOSAP unit are consistent with what would be obtained with the sort of electronics NPL would normally use for this type of measurement.

4 ANALYSIS

4.1 Initial processing of the data

As a first step in analysing the data all the scaler counts were transferred to an Excel workbook where dead-time corrections were performed for the counts from the SP9 counter and for the counts from the fission chambers. Ratios of the dead-time corrected individual SP9 counts, N, to those for the two fission chambers were calculated. The fission chamber counts are designated M_C for the column fission chamber, FC_C, and M_H for the chamber close to the access hole, FC_H. Means, standard deviations and values for the standard error of the mean were then calculated for the number of cycles involved in each measurement, i.e. mean values were obtained for N, M_C, M_H, N/M_C, and N/M_H. The demand level, D, is constant for a measurement so a value for N/D is easily derived. The approach of calculating N/M_C and N/M_H values for individual cycles and then deriving a mean of these ratios was taken because any variation in the fluence rate during the cycles will result in variations in the individual N, M_C, and M_H values, but should not affect the ratios. There was, however, little or no indication of variation of the fluence over the majority of the measurements. The above analysis was performed for all configurations of the SP9 counters and moderating sphere, and also for these configurations enclosed in the appropriate cadmium cover provided.

4.2 Monitor stability

To obtain a value for the fluence response of the SP9 detector, for example from the mean ratio for N/M_C, requires a calibration of the fission counter monitor in terms of neutron fluence per fission chamber count M_C. This is obtained from the gold foil measurement. Because this measurement is made at one particular time, and for one particular demand level, it is essential that the monitors are stable. To check the performance of the monitors their ratios were investigated both as a function of demand level and of time. Figure 4 shows the ratios of M_H/M_C, M_C/D, and M_H/D as a function of demand. In all cases the uncertainties in the ratios increase as the demand increases because of the uncertainty in the dead-time correction. All the ratios are for measurements with an SP9 counter, except for one of the measurements at a demand of 10 which was that for the irradiation of the gold foils. Note that the majority of measurements were made for demand levels in the range 0.3 to 3.

The ratio M_H/M_C is constant within the uncertainties over the range of demand levels, indicating that these two monitors agree very well with each other. There is even an indication that the assigned uncertainties, due mainly to statistics at low demand level and the uncertainty in the dead-time correction at higher demand levels, might be a little large in view of the level of agreement.

For the ratio M_C/D the values are reasonably constant except for the one at the lowest demand value of 0.1 where there is a clear suggestion that either M_C is too low or D is too high. There is some indication that this problem may also be present in the data for the next highest demand level of 0.3. Overall, the results for this ratio when viewed for all demand levels, suggest that the uncertainties may be slightly underestimated, but in view of the fact that the plot of the data for M_H/M_C indicates the opposite, i.e. that the fission chamber uncertainties may be slightly overestimated, no changes were made to the uncertainties in M_C/D.

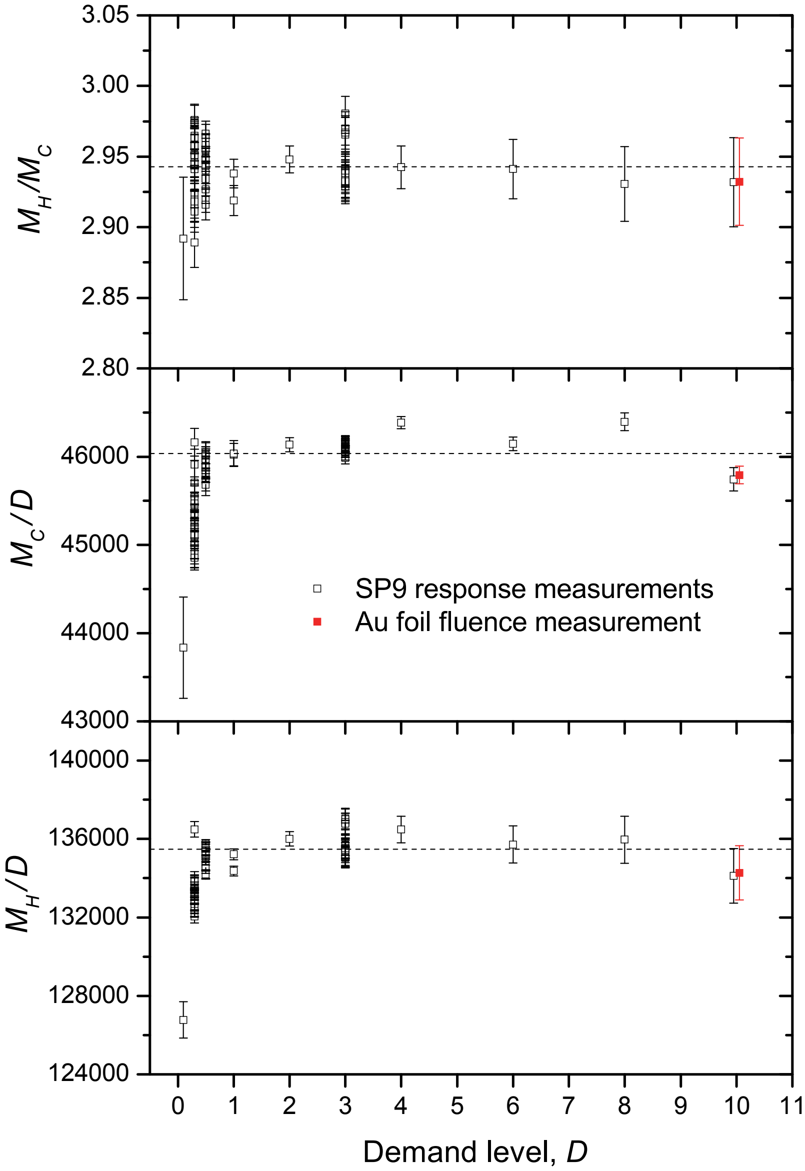

Figure 4. Ratios of monitor readings as a function of demand level for all the measurements performed. The dotted horizontal lines indicate mean values for these ratios over the range of demand values from 0.5 to 10.

The bottom plot in Figure 4 shows the data for M_H/D. These are similar to those for M_C/D, indicating a constant value for demand levels between 0.5 and 10, but with indications that either M_H is too low or D is too high below a demand of 0.5.

From the data in Figure 4 it can be concluded that all three monitors perform well over the range of demands from 0.5 to 10, and that any one could be chosen. The consistency of M_H/M_C over the entire range of demand levels would indicate that the low values for M_C/D and M_H/D for demands below 0.5 are due to problems with the demand as a monitor in this region, however, further data on this issue is available from the variation of the results for the SP9 counters with demand and this is discussed in section 4.3.

In Figure 5 the data for M_C/D are shown, for all demand levels used, as a function of time covering the whole period of the measurements. This figure highlights the consistency of this ratio for demand levels of 0.5 and above and the fact that there is definitely a problem with one of the monitors for the lowest demand level, i.e. 0.1. Except for a couple of data points, the results for data taken at a demand of 0.3 indicate that there may also be a problem with one of the monitors at this demand level. The value of M_C/D is roughly 2% lower for this demand than the average for higher demands. There is no indication of variation of the monitor ratios over the period of the measurements. The data for M_H/D provides similar evidence of the stability of the monitors with time.

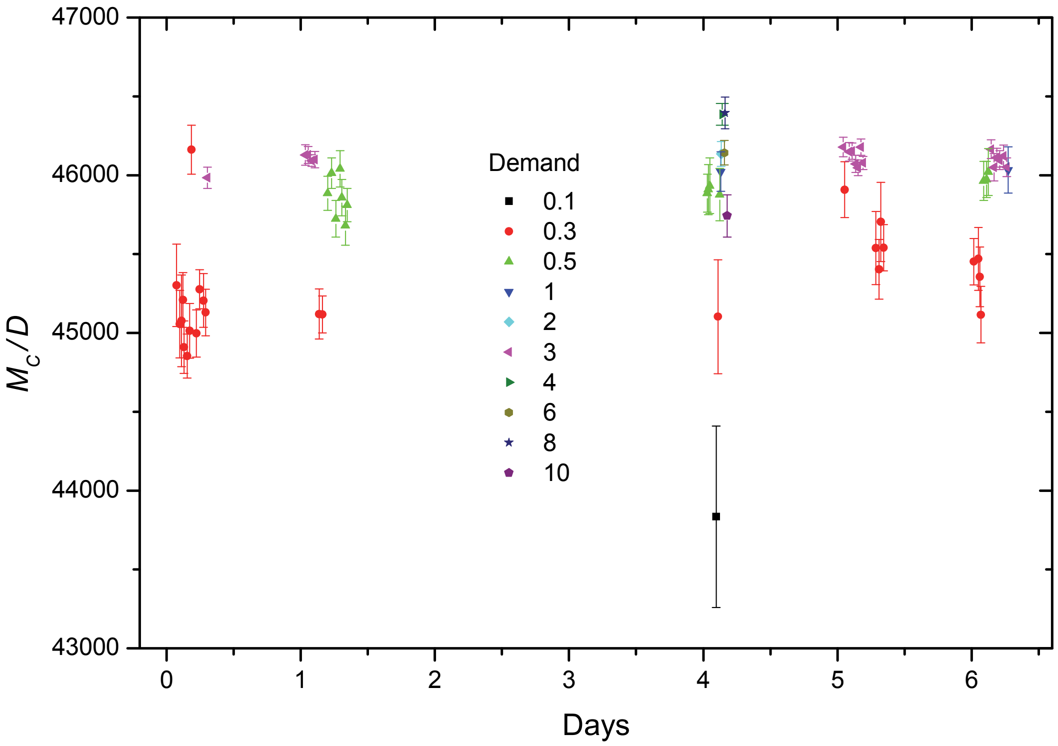

Figure 5. Variation of the ratio M_C/D with time from the first measurement.

4.3 The SP9 counter dead-time when using the AIOSAP electronics

If all corrections that need to be applied to the SP9 counts and to the monitor readings have been applied and are correct, then the quantity 'SP9 counts per unit monitor reading' should be constant for all demand levels for a particular SP9 counter configuration. Figure 6 shows this ratio for the three monitors for a series of measurements which were taken over a range of demand levels for a fixed SP9 counter configuration (bare detector mounted parallel to the neutron beam). Dead-time corrections to the SP9 counts were applied assuming a dead-time per pulse from the AIOSAP unit of 7.2 ± 0.9 µs as specified in the protocol. The conventional equation for a non-extending dead time, eq. (9), was used to relate the corrected counts N to the measured counts N' via the measured count rate R' (equal to N' divided by the measurement time T), and the dead-time per pulse τ.

$$N = \frac{N'}{(1 - R' \cdot \tau)} \tag{9}$$

The rather large uncertainties at the higher demand levels are a result of the large dead-time corrections applied to the SP9 counts (42% for a demand of 10). This correction is common to all three sets of data, i.e. they are correlated. This explains why the results for the different monitors agree better than would be expected from a simple consideration of the error bars.

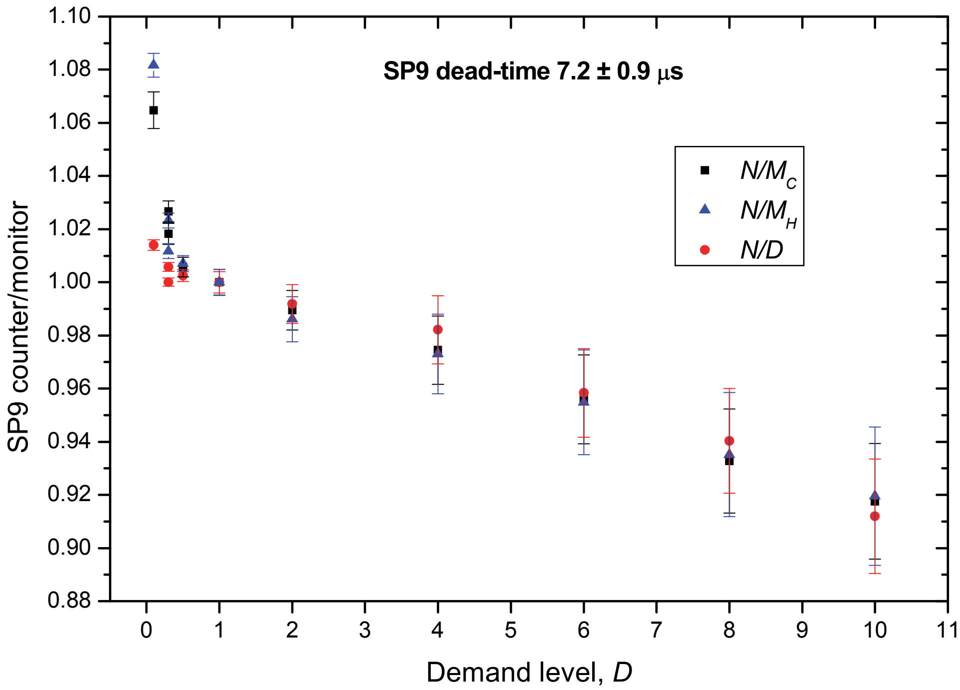

Figure 6. Variation of the counts, N, per unit monitor reading, M_C, M_H or D, as a function of demand for the 200 kPa SP9 counter mounted vertically free in air. The three sets of data are all normalised to unity for the measurement at a demand of 1.0.

In spite of the rather large uncertainties at higher demand levels, resulting from the uncertainty in the dead-time, it is clear that the data are not consistent, and the indications are that the dead-time of 7.2 µs is not applicable, certainly not at the higher demand levels. A check using a double pulser, where the time between pulses could be varied over a range of several µs, indicated that the specified dead-time of 7.2 µs was correct at low count rates. The two-source method was then used to measure the dead-time at higher count rates, similar to those seen at the higher demand levels. Values were obtained which were larger than 7.2 µs. For a combined rate from the two sources that was similar to that at a demand of 10 the dead-time was measured as 8.8 µs. For lower rates the dead time was smaller, but still greater than 7.2 µs. The indications are thus that the dead-time may be rate dependent. Because the two source method uses readings at different count rates to derive the dead-time, its results cannot be relied upon if the dead-time is truly rate dependent, but it does give a clear indication that the dead-time was not 7.2 µs at the higher rates.

It is possible that the dead-time is extending rather than non-extending. An expression relating measured counts to the true number of events which occurred can be written for the case of extending dead-time, but it involves the term $e^{-R\tau}$ where R is the true count rate which is unknown. Allowance was therefore made for the apparently varying dead-time using eq. (10)below:

$$N = \frac{N'}{(1 - R' \cdot (1 + R'/R_0) \cdot \tau)} \qquad (10)$$

where R_0 is a constant adjusted manually to make the values of the SP9 counts/monitor constant over the range of demand values used in the measurements. The results are shown in Figure 7.

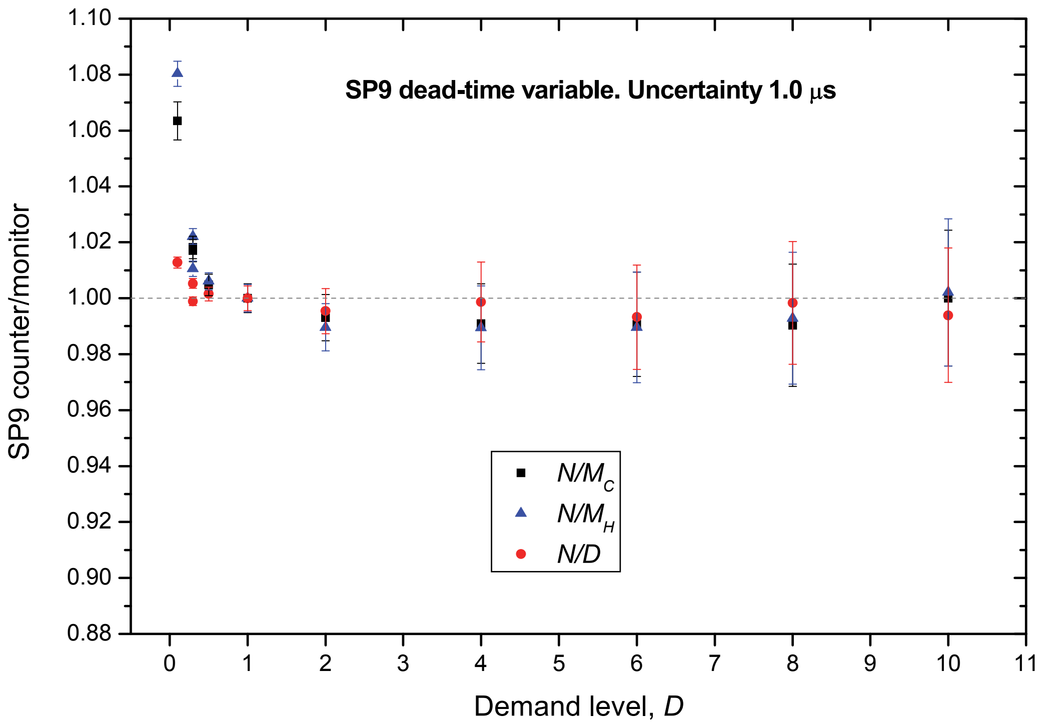

Figure 7. As for Figure 6 but with a variable dead-time.

The optimum value for R_0 was found to be 16000 s^{-1} which resulted in a dead-time of 9.2 μs for a demand of 10 where the SP9 count rate was about 32,000 s^{-1}. For a demand of 0.5 the dead-time was still 7.2 μs. It can be seen that, for this value of R_0, the ratios of the SP9 counts to the various monitor readings are all consistent, within the uncertainties, over the range of demands from 0.5 to 10. This approach has no underlying physical justification. It simply provides a way of performing dead-time corrections which ensure that the ratios of SP9 counts per unit monitor reading have the correct properties as a function of demand level. The assumption of a fixed dead-time of 9.2 μs gave much better overall consistency of the SP9 counts per unit monitor values than a dead-time of 7.2 μs, but not as good consistency as the varying dead-time approach. No reason for the problem with the dead-time of the AIOSAP electronics has yet been discovered. It is possible that it was a result of the combination of the AIOSAP with the width/delay unit used to provide input to the scaler system. Luckily the effect on the final results for the response values is small since the vast majority of the measurements were made at low demand levels where the dead-time corrections are small. To allow for the inexact knowledge of the dead-time an uncertainty of ±1 μs was assigned.

4.4 Data at demand levels of 0.3 or lower

At a demand of 0.1 the ratios of the SP9 counts to the three monitors are inconsistent with the values at higher demand levels, and in view of the problems identified at this demand level when ratios of monitor readings were compared, the single measurement at this demand was not included in the final results.

The data for a demand of 0.3 in Figure 5 and Figure 7, suggest that there may also be a slight problem with the monitoring at this demand level. To investigate this matter results for SP9 counts per unit monitor taken for a demand of 0.3 were compared with data taken at higher demand levels wherever such data were available for a particular detector configuration. Results are shown in Table 2.

Table 2. Ratio of results for SP9 counts, *N*, per unit monitor, *M*, for measurements at a demand of 0.3 to the corresponding results for a demand greater than 0.3.

Configuration	$(N/M)_{D=0.3}/(N/M)_{D>0.3}$		
	FC_C	FC_H	Demand
200 kPa SP9 bare vertical	1.017	1.014	1.001
20 kPa SP9 bare vertical	1.020	1.029	1.007
20 kPa SP9 bare horizontal	1.015	1.019	0.991
Mean value =	1.017	1.021	1.000
Correction factor =	0.991	0.989	1.000
Uncertainty in correction factor =	0.009	0.010	0.009

It appears from Table 2 that $(N/M)_{D=0.3}$ is roughly 2% higher than $(N/M)_{D>0.3}$ for both fission counters, but the ratio $(N/M)_{D=0.3}/(N/M)_{D>0.3}$ is unity within the uncertainties, which are of the order of 1%, when the demand is the monitor. This is a slightly surprising result as both fission chambers would be expected to act as very stable monitors when the fluence rate is changed, whereas the demand value itself is simply a setting for the electronics which controls the overall operation of the thermal pile. Nevertheless, the data point to small problems with the fission chambers at low levels and a correction factor was applied so that the results for *N/M* at a demand of 0.3 were decreased by half the difference between the measured value for $(N/M)_{D=0.3}/(N/M)_{D>0.3}$ and the value expected for a perfect monitor, i.e. unity. The implications that M_C and M_H are low at a demand of 0.3, and are low by roughly the same amount, explains the data for this demand level as shown in Figure 4.

For the cases where the fission chambers were used as monitors uncertainties were assigned to the correction factors which were large enough to cover both the measured value for the ratio and the ‘perfect monitor’ situation, i.e. a ratio of 1.0. From the data for the demand as monitor it appears that the demand is a good monitor right down to a level of 0.3. The correction factor was therefore unity; however, an uncertainty component was included to cover any possible problems with the demand as monitor and was set to cover the range ratios shown in Table 2.

4.5 Background in the SP9 counters

A check of the background count rates in the two SP9 counters with all neutron-producing equipment switched off revealed an almost zero rate, which was completely negligible compared to the count rates recorded during the measurements. However, with the accelerator beam present in the thermal pile there is the possibility of a neutron background in the room which is not due to deuterons striking the neutron-producing targets in the pile, and which is thus not accurately monitored by the demand level and the fission chambers. One possible mechanism would be from neutron production at the tantalum stop situated where the beam enters the pile, see Figure 1. There must be some deuteron build-up on the tantalum with time. This room background is very difficult to measure, and may vary with the beam current settings. If such a background exists it is likely to be most evident at low count rates in the SP9, and so to investigate its presence the data for the SP9 counts per unit demand have been plotted against demand, see Figure 8. This is essentially the same data as plotted in Figure 7, except that, for clarity, the error bars show only the statistical uncertainties with no contribution for uncertainty in the dead-time.

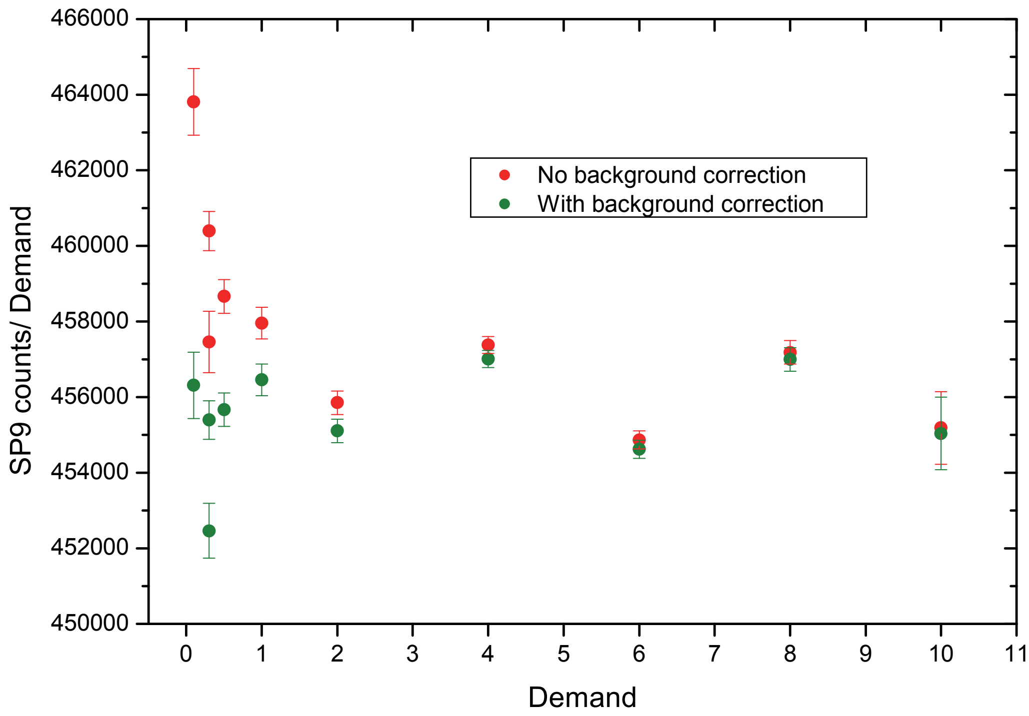

Figure 8. Variation of 200 kPa SP9 counts per unit demand with demand level.

With no background correction the ratio SP9/demand increases as the demand decreases. By applying a background subtraction it was possible to make the ratio reasonably constant as a function of demand. The actual background value was obtained by varying it until the ratio was constant. The effect of this background is small, being of the order of 1% at a demand of 0.3, and becoming a smaller percentage still at higher demands values. (It is evident from Figure 8 that the statistical uncertainty alone is not enough to account for the variations in the ratios as a function of demand and some other component must be present possibly associated with the division of the beam between targets and the tantalum stop.)

The data in Figure 8 indicates the presence of a room background. However, other data do not always support this. Column 4 in Table 2 records ratios of SP9 counts per unit demand for demand levels of 0.3 and levels >3.0. These are reasonably consistent. In one case the value at 0.3 is smaller than at higher demands. In view of the fact that a correction is made for *N/M* at a demand of 0.3 being larger than at higher demands when the fission chambers were used as monitors, see section 4.4, and the fact that most of the data were taken at demands greater than 0.3, no corrections have been made for room background. Nevertheless, an additional uncertainty component of 0.5% has been added to the uncertainty budget to cover possible background effects.

The overall conclusion from the various checks described in section 4 is that, for the highest levels of accuracy, there may be some problems with the monitors at very low demand levels; however, uncertainties have been assigned which allow for these problems.

4.6 Calibration of the monitors

The various investigations of monitor performance indicate that, after the small corrections outlined in section 4.4 have been made to data taken at a demand of 0.3, any of the three monitors can be used with equal validity. (The single datum at a demand of 0.1 is clearly unreliable and was excluded.) For the final results a mean of the data for all three monitors was therefore taken.

As already noted, calibration of the monitors was performed, towards the middle of the measurement campaign, by irradiating a pair of gold foils, one bare and one under cadmium cover. The irradiation was performed for 3 hours at a demand level of 10, and the foil activity determined immediately afterwards. From Figure 4 it can be seen that, although the value for M_C/D was a bit low for the calibration run, there is no valid reason not to accept the results of this calibration for all three monitors. Values for the fluence rates during the monitor calibration and the calibration coefficients, i.e. $\Phi / M_{\Phi i}$, where $M_{\Phi i}$ is the monitor count for monitor *i* during the fluence calibration which gave a fluence value Φ, are given in Table 3. (The index i would be *C* for FC_C, *H* for FC_H and *D* for the demand level.)

Table 3. Values for the fluence rates during the monitor calibration and the fluence per unit monitor for the three monitors.

Quantity	Fluence rate (cm^{-2} s^{-1})	Fluence per unit monitor reading $\Phi / M_{\Phi i}$ (cm^{-2} M^{-1})		
		FC_C	FC_H	Demand
nv_0	1.495×10^4	3.264	1.113	1494.9
$n_{th}v_0$	1.479×10^4	3.231	1.102	1479.4
$n_m v_0$	1.460×10^4	3.188	1.087	1459.8
$n_{th}\overline{v}_{th}$	1.763×10^4	3.851	1.313	1763.0
$n_m\overline{v}_m$	1.706×10^4	3.726	1.270	1705.9

As a check of the calibration the value obtained for the calibration coefficient for FC_C, was compared with earlier measurements when using gold foils positioned at the height used in this experiment (1.6 m). Monitor FC_C is the one usually employed for irradiations in the thermal column. The results are shown in Table 4 and show very good consistency. Nevertheless, the best value to use for this work is that derived during the present measurement campaign as the fission chamber discriminator setting can vary slightly with time over periods in excess of a few days.

Table 4. Earlier FC_C calibrations with gold foils at a reference height of 1.6 m.

Measurement date	Fluence $n_{th}v_0$ per unit FC_C count (cm^{-2} M^{-1})
5th April 2006	3.211
13th June 2006	3.219
19th February 2007 (present measurements)	3.231

4.7 Measurements for the various configurations

The sub sections below give the results for the fluence response of the various detector configurations, for each fluence monitor used, and for two representations of the fluence rate, $\phi_W(th) = n_{th}v_0$ and $\phi(th) = n_{th}\overline{v}_{th}$. For each monitor, *i*, the responses, $R_{\text{W-NPL}i}$ and $R_{\text{NPL}i}$, were calculated using eqs (11) and (12) below

$$R_{\text{W-NPL}i} = \frac{\left(N / M_{Ni} - k^{(\text{Cd})} N^{(\text{Cd})} / M_{Ni}^{(\text{Cd})}\right)}{\left(\Phi_w(th) / M_{\Phi i}\right)} \tag{11}$$

and

$$R_{\text{NPL}i} = \frac{\left(N / M_{Ni} - k^{(\text{Cd})} N^{(\text{Cd})} / M_{Ni}^{(\text{Cd})}\right)}{\left(\Phi(th) / M_{\Phi i}\right)} \tag{12}$$

where:

$R_{\text{W-NPL}i}$	is the response, as measured with monitor *i,* in the sub-cadmium-cut-off Westcott fluence of the NPL thermal column beam,
$R_{\text{NPL}i}$	is the response, as measured with monitor *i,* in the sub-cadmium-cut-off true fluence of the NPL thermal column beam,
N / M_{Ni}	is the bare detector count per monitor *i* count (or reading in the case of the demand as monitor),
$N^{(\text{Cd})} / M_{Ni}^{(\text{Cd})}$	is the detector count per monitor *i* count for the detector under cadmium,
$k^{(\text{Cd})}$	is a correction factor for attenuation of the neutrons above the cadmium-cut-off energy in the cadmium cover,
$\Phi_W(th) / M_{\Phi i}$ and $\Phi(th)$	are the calibration coefficients for monitor *i* for $\phi_W(th)$ and $\phi(th)$.

Values for the cadmium cover correction factor $k^{(Cd)}$ were calculated using the Monte Carlo code MCNP. For both the bare detectors the value was estimated to be 1.000 ± 0.005, and for the detectors within the polyethylene sphere the factor was 0.990 ± 0.005[10].

The values of N / M_{Ni} and $N^{(\text{Cd})} / M_{Ni}^{(\text{Cd})}$ were in most cases derived as a mean of several measurements, sometimes at different demand levels. Uncertainties for the mean values were calculated taking into account statistics (in the SP9 counts and the monitor where applicable), the uncertainty in the dead-time corrections, and those due to the correction for monitoring inconsistency at a demand of 0.3 where necessary. To determine the uncertainties in $R_{\text{W-NPL}i}$ and $R_{\text{NPL}i}$ the uncertainties in N/M_{Ni} and $N^{(\text{Cd})}/M_{Ni}^{(\text{Cd})}$ were combined with those in the relevant $k^{(\text{Cd})}$ factor and those in the monitor counts $M_{\Phi i}$ during the fluence calibration. The aim was to exclude uncertainties that are common to measurements with all three monitors. Thus, the uncertainty in the fluence Φ during the monitor calibration was excluded. The use of mean values for N/M_{Ni} and $N^{(\text{Cd})}/M_{Ni}^{(\text{Cd})}$ from measurements at different demand levels makes it impossible to separate out the dead-time correction uncertainty from the statistical uncertainty in a final uncertainty budget. There is also the fact that the results are correlated because the same SP9 counts are used in the analysis for the three monitors, however, the process described above of deriving mean values for the ratios N/M_{Ni} and $N^{(\text{Cd})}/M_{Ni}^{(\text{Cd})}$ makes this correlation inevitable.

To quantify the level of agreement between results obtained with the different monitors a χ^2/ν value was calculated for each data set using eq. (13):

$$\chi^2/\nu = \sum_{i=1}^{n} \frac{(x_i - \overline{x})^2/\sigma_i^2}{(n-1)} \tag{13}$$

where:

x_i	is the result, $R_{\text{W-NPL}i}$ or $R_{\text{NPL}i}$, derived using a particular monitor,
$\overline{x}$	is the mean result,
σ_i	is the uncertainty in x_i, and
n	is the number of results, 3 in this case.

For each configuration, averaged responses $R_{\text{W-NPL}}$ and R_{NPL}, derived from a weighted mean of the responses $R_{\text{W-NPL}i}$ and $R_{\text{NPL}i}$ obtained with the three monitors, are presented. The uncertainty σ_m quoted for the mean is the larger of the values obtained from the spread of the results as derived from eq. (14):

$$\sigma_m = \sqrt{\frac{\sum_{i=1}^{n}(x_i - \overline{x})^2 w_i}{(n-1)\sum_{i=1}^{n} w_i}} \tag{14}$$

or from the value obtained by combining the individual uncertainties using eq. (15):

$$\sigma_m = \sqrt{1\Big/\sum_{i=1}^{n} w_i} \tag{15}$$

where:

w_i	is the weight for each response given by $w_i = 1/\sigma_i^2$.

Because the SP9 counts are common to all three $R_{\mathrm{NPL}i}$ values there are correlations in the data for which allowance should in principle be made. The SP9 counting uncertainties are, however, small and in view of the rather pessimistic approach outlined above of taking the largest value from eqs (14) and (15), it was felt that the correlations could be neglected.

4.7.1 200 kPa SP9, parallel to the beam, no polyethylene moderator sphere

For this configuration bare detector measurements were performed at 10 different demand levels covering the range from 0.1 to 10, although the datum at a demand of 0.1 was not included in the final results. The mean values for the three monitors are shown in Table 5. All the results have been corrected for the response to epi-cadmium neutrons via a cadmium-cover measurement. However, this measurement was made at a demand of 0.3 so required a small correction (see section 4.4).

The results for the three monitors are completely consistent within the uncertainties quoted in Table 5. A value of 0.4 was obtained for the χ^2/ν defined in eq. (13).

Table 5. Results for 200 kPa SP9, parallel to the beam, no polyethylene moderator.

Monitor	Response $R_{\mathrm{W\text{-}NPL}i}$ to the sub-cadmium fluence in the Westcott convention $n_{th}v_0$ (cm^2)	Response $R_{\mathrm{NPL}i}$ to the true sub-cadmium fluence $n_{th}\overline{v}$ (cm^2)
FC_C	3.020 ± 0.36%	2.534 ± 0.36%
FC_H	3.017 ± 1.1%	2.532 ± 1.1%
Demand	3.032 ± 0.29%	2.544 ± 0.29%
Weighted mean	3.0269 ± 0.22%	2.5399 ± 0.22%

4.7.2 200 kPa SP9, perpendicular to the beam, no polyethylene moderator sphere

Five measurements were performed with the counter bare for this configuration and 4 with it under cadmium. All measurements were made at a demand of 0.3 and appropriate corrections were made for the monitor inconsistency at this demand (see section 4.4). As can be seen from Table 6, there is extremely good agreement between the three monitors with a χ^2/ν value of 0.2.

For this configuration results were also obtained, at a demand level of 0.3, using NPL electronics for the SP9 counter. The values for the responses were 1.0% higher when averaged over the three monitors and the derived uncertainty was 0.61%. The difference is thus within the uncertainties quoted. Furthermore, the measurements were made five days apart, so there may be additional uncertainties, e.g. for variation in the calibration of the monitors with time, which should be added to the values quoted above of 0.61% for the NPL electronics and 0.57% for the AIOSAP electronics.

Table 6. Results for 200 kPa SP9, perpendicular to the beam, no polyethylene moderator.

Monitor	Response $R_{\text{W-NPL}i}$ to the sub-cadmium fluence in the Westcott convention $n_{th}v_0$ (cm^2)	Response $R_{\text{NPL}i}$ to the true sub-cadmium fluence $n_{th}\overline{v}$ (cm^2)
FC_C	3.303 ± 0.82%	2.771 ± 0.82%
FC_H	3.273 ± 1.4%	2.746 ± 1.4%
Demand	3.290 ± 0.95%	2.760 ± 0.95%
Weighted mean	3.293 ± 0.57%	2.763 ± 0.57%

The cadmium ratio for measurements with the bare 200 kPa SP9 counter was about 65 for both parallel and perpendicular orientations of the counter relative to the beam

4.7.3 SP9 20 kPa parallel to the beam no polyethylene moderator sphere

For this configuration measurements of the bare SP9 detector were made at demands of 0.3 and 3.0, and an under-Cd measurement at a demand of 3.0. The data at a demand of 0.3 were corrected as described in section 4.4 and an average taken of all the measurements. The results are given in Table 7. No measurements were made with NPL electronics. This is a data set for which agreement between the results using the three different monitors was relatively poor, with a χ^2/ν value of 1.8. However, the uncertainty in the mean value was taken from the spread of the results so allowance for the spread is made in the quoted uncertainty.

Table 7. Results for 20 kPa SP9, parallel to the beam, no polyethylene moderator.

Monitor	Response $R_{\text{W-NPL}i}$ to the sub-cadmium fluence in the Westcott convention $n_{th}v_0$ (cm^2)	Response $R_{\text{NPL}i}$ to the true sub-cadmium fluence $n_{th}\overline{v}$ (cm^2)
FC_C	0.3662 ± 0.32%	0.3073 ± 0.32%
FC_H	0.3627 ± 1.1%	0.3043 ± 1.1%
Demand	0.3684 ± 0.24%	0.3091 ± 0.24%
Weighted mean	0.3675 ± 0.25%	0.3083 ± 0.25%

4.7.4 SP9 20 kPa perpendicular to the beam no polyethylene moderator sphere

Measurements were performed at demand levels of 0.3 and 3.0, and after correction of the lower demand level data mean values were derived. The results are shown in Table 8. Again the χ^2/ν value was high at 2.1, but allowance has been made for this in the uncertainty quoted for the mean which was derived from the spread of the results.

Table 8. Results for 20 kPa SP9, perpendicular to the beam, no polyethylene moderator.

Monitor	Response $R_{\text{W-NPL}i}$ to the sub-cadmium fluence in the Westcott convention $n_{th}v_0$ (cm^2)	Response $R_{\text{NPL}i}$ to the true sub-cadmium fluence $n_{th}\overline{v}$ (cm^2)
FC_C	0.3918 ± 0.31%	0.3287 ± 0.31%
FC_H	0.3872 ± 1.1%	0.3248 ± 1.1%
Demand	0.3943 ± 0.29%	0.3308 ± 0.29%
Weighted mean	0.3929 ± 0.30%	0.3296 ± 0.30%

Measurements made with NPL electronics, at a demand level of 3.0, gave results which were 0.62% lower. The measured uncertainty in these results was 0.25% and in view of the 0.25% uncertainty in the results with the AIOSAP electronics the two measurements almost agree within the uncertainties. However, the measurements were made on different days, so there will be additional uncertainty components.

The cadmium ratio for measurements with the bare 20 kPa SP9 counter was about 82 for both parallel and perpendicular orientations of the counter relative to the beam.

4.7.5 SP9 200 kPa parallel to the beam with polyethylene moderator sphere

The measurements were performed at a demand level of 0.5 and the results are shown in Table 9. There was remarkable agreement between the values obtained with the three different monitors and the χ^2/ν value was 0.4.

Table 9. Results for 200 kPa SP9, parallel to the beam, with polyethylene moderator.

Monitor	Response $R_{\text{W-NPL}i}$ to the sub-cadmium fluence in the Westcott convention $n_{th}v_0$ (cm^2)	Response $R_{\text{NPL}i}$ to the true sub-cadmium fluence $n_{th}\overline{v}$ (cm^2)
FC_C	1.5429 ± 0.55%	1.2946 ± 0.55%
FC_H	1.528 ± 1.1%	1.282 ± 1.1%
Demand	1.5439 ± 0.43%	1.2955 ± 0.43%
Weighted mean	1.5422 ± 0.32%	1.2940 ± 0.32%

When NPL electronics were used, again at a demand level of 0.5, the results were 0.62% higher with excellent agreement for the three monitors and an overall uncertainty of 0.38%. The difference between the results with NPL electronics and AIOSAP electronics is thus within the uncertainties quoted here.

4.7.6 SP9 200 kPa perpendicular to the beam with polyethylene moderator sphere

For this measurement, as for the previous measurement with the polyethylene sphere, a demand level of 0.5 was used for both the total and under-cadmium measurement, and the results are shown in Table 10. The χ^2/ν value was 0.3. No measurements were made with NPL electronics.

Table 10. Results for 200 kPa SP9, perpendicular to the beam, with polyethylene moderator.

Monitor	Response $R_{\text{W-NPL}i}$ to the sub-cadmium fluence in the Westcott convention $n_{th}v_0$ (cm^2)	Response $R_{\text{NPL}i}$ to the true sub-cadmium fluence $n_{th}\bar{v}$ (cm^2)
FC_C	1.580 ± 0.79%	1.325 ± 0.79%
FC_H	1.562 ± 1.2%	1.310 ± 1.2%
Demand	1.574 ± 0.77%	1.320 ± 0.77%
Weighted mean	1.5741 ± 0.50%	1.3208 ± 0.50%

The cadmium ratio for measurements with the 200 kPa SP9 counter in the moderator was 3.9 for both parallel and perpendicular orientations of the counter relative to the beam.

4.7.7 SP9 20 kPa parallel to the beam with polyethylene moderator sphere

Results for measurements in this configuration are shown in Table 11. Measurements were made with AIOSAP electronics and NPL electronics all at a demand level of 3.0. The χ^2/ν value for the AIOSAP measurements was 1.5, but nevertheless the uncertainty on the final weighted mean, calculated from the spread of the data, was still only 0.30%

Table 11. Results for 20 kPa SP9, parallel to the beam, with polyethylene moderator.

Monitor	Response $R_{\text{W-NPL}i}$ to the sub-cadmium fluence in the Westcott convention $n_{th}v_0$ (cm^2)	Response $R_{\text{NPL}i}$ to the true sub-cadmium fluence $n_{th}\bar{v}$ (cm^2)
FC_C	0.2536 ± 0.38%	0.2128 ± 0.38%
FC_H	0.2530 ± 1.2%	0.2123 ± 1.2%
Demand	0.2558 ± 0.34%	0.2146 ± 0.34%
Weighted mean	0.2547 ± 0.30%	0.2137 ± 0.30%

The results with the NPL electronics were on average 5.2% higher. This is a long way outside the measurement uncertainties and a review of the data revealed no obvious reason for this difference. However, some support for the AIOSAP results, and a reason to suspect those obtained with the NPL electronics, can be derived from a comparison with the results (4.7.8) for the 20 kPa SP9 counter in the moderator sphere with the SP9 counter perpendicular to the beam rather than parallel. The results obtained with the AIOSAP electronics for these two configurations are only 0.8% different. A similar comparison for the 200 kPa counter gave a difference of 1.5% between perpendicular and parallel. Because of the moderation in the sphere these configurations would not be expected to give significantly different results so the similarity of the results with the AIOSAP electronics suggests that there were no problems with these measurements.

4.7.8 SP9 20 kPa perpendicular to the beam with polyethylene moderator sphere

Table 12 shows the results for measurements with this configuration. Measurements were only made with AIOSAP electronics, all at a demand level of 3.0. The χ^2/ν value was 1.3, and the uncertainty on the final weighted mean, calculated from the spread of the data, was 0.29%

Table 12. Results for 20 kPa SP9, perpendicular to the beam, with polyethylene moderator.

Monitor	Response $R_{\text{W-NPL}i}$ to the sub-cadmium fluence in the Westcott convention $n_{th}v_0$ (cm^2)	Response $R_{\text{NPL}i}$ to the true sub-cadmium fluence $n_{th}\overline{v}$ (cm^2)
FC_C	0.2556 ± 0.39%	0.2144 ± 0.39%
FC_H	0.2553 ± 1.2%	0.2142 ± 1.2%
Demand	0.2576 ± 0.34%	0.2162 ± 0.34%
Weighted mean	0.2567 ± 0.29%	0.2154 ± 0.29%

The cadmium ratio for measurements with the 20 kPa SP9 counter in the moderator was 4.3 for both parallel and perpendicular orientations of the counter relative to the beam.

4.8 Summary of the analysis

In general the results obtained using the three different monitors agreed within the uncertainties. The average value of χ^2/ν was almost exactly 1.0 although it might be expected to be slightly lower in view of the correlations introduced by the fact that the SP9 counts were common in all cases.

An inspection of the average values of the differences between the results for a particular monitor and the mean for all three revealed that, for the AIOSAP electronics, the results with FC_H were on average 0.79% below the mean, and in all cases were the lowest result. However, there is a relatively large uncertainty (~1%) in $M_{\Phi i}$ for this monitor, caused by the large, 15%, dead-time correction during the fluence calibration. Overall, the three data sets still agree as well as could be expected in view of the uncertainties. For the other two monitors the results are sometimes larger and sometimes smaller than the mean as would be expected on the basis of statistics. The results for the NPL electronics were more consistent with a χ^2/ν of only 0.4, so the evidence for an error in $M_{\Phi i}$ for monitor FC_H is not conclusive and results for all three monitors were retained.

5 RESULTS

5.1 Correction for the results in a Maxwellian distribution with *kT* = 25.3 meV

No two thermal fields are ever likely to be exactly the same, particularly when, as in the present comparison exercise, they are produced in a variety of different ways. For this reason the organisers of the comparison have requested that: "The participants shall determine the response R_{ref} of the counters for a homogeneous unidirectional irradiation with neutrons with a Maxwellian fluence distribution $\Phi_E^{(\text{ref})}$ characterised by a temperature parameter $kT = 25.3$ meV". The reference Maxwellian field is described by the expression:

$$\frac{\Phi_E^{(ref)}\,\mathrm{d}E}{\Phi^{(ref)}} = \left(\frac{E}{kT}\right)\exp\left(-\frac{E}{kT}\right)\frac{\mathrm{d}E}{kT} \tag{16}$$

where:

- $\Phi_E^{(ref)}$ is the fluence at neutron energy E,
- $\Phi^{(ref)}$ is the total fluence in the distribution,
- k is Boltzmann's constant, and
- T is the temperature of the Maxwellian, $T = 20.4^{\circ}$C for $kT = 25.3$ meV.

The beam from the thermal column is sufficiently plane-parallel to satisfy the requirement of being unidirectional, but the results still need to be corrected to those which would have been obtained in the designated reference spectrum.

The spectrum Φ_E in the NPL thermal column field, in the region below the cadmium cut-off energy, can be expressed(11) as :

$$\frac{\Phi_E \mathrm{d}E}{\Phi} = C_M\left(\frac{E}{kT}\right)\exp\left(-\frac{E}{kT}\right)\frac{\mathrm{d}E}{kT} + C_{1/E}\,\frac{1}{\ln(E_{Cd}/E_\Delta)}\frac{\mathrm{d}E}{E}\Delta \tag{17}$$

where:

- C_M is the fraction of the total sub-cadmium fluence in the Maxwellian peak,
- $C_{1/E}$ is the fraction of the total sub-cadmium fluence with a $1/E$ distribution,
- E_{Cd} is the cadmium cut-off energy,
- E_Δ is the lower energy limit of the $1/E$ distribution, and
- Δ is a function which is 1 between E_Δ and E_{Cd} and 0 outside this region.

Both the expression for the Maxwellian and the $1/E$ distribution are normalised to unity so the fractions of the fluence in the two distributions are given by the factors C_M and $C_{1/E}$. The values of these factors, and of the effective temperature T, were derived from gold foil measurements, and were:

$C_{1/E} = 0.0324$
$C_M = (1 - C_{1/E}) = 0.9676$
$T = 22.6^{\circ}$C above the temperature of the moderator, thus $kT = 27.2$ meV.

Using equations (16) and (17) the correction factor k_1 for the spectral distribution can be calculated for any instrument with response function *r(E)* from:

$$k_1 = \frac{\int_0^{\infty} \Phi_E^{(ref)} / \Phi^{(ref)} \, r(E) \mathrm{d}E}{\int_0^{E_{Cd}} \Phi_E / \Phi \, r(E) \mathrm{d}E} \tag{18}$$

A FORTRAN program was written to calculate the correction factors for the various configurations using NAG Library routines(12) to perform the integrations. Response functions were provided by the comparison organiser for all four detector configurations used. The results of the calculations are presented in Table 13. No indication was given whether these response functions were calculated for neutron incidence parallel to the stem of the SP9 detector or perpendicular to the stem. In view of the relatively small size of the k_1 corrections this detail is assumed unimportant.

Table 13. Factors k_1 used to correct measured responses to those expected in a pure room-temperature Maxwellian distribution.

Configuration	Response to actual sub-cadmium field	Response in Maxwellian with kT = 25.3 meV	Factor k_1 = Ratio Pure Maxwellian / Actual field
SP9 200 kPa no moderator	0.840	0.868	1.042 ± 0.012 (1.2%)
SP9 20 kPa no moderator	0.834	0.862	1.053 ± 0.016 (1.5%)
SP9 200 kPa with moderator	1.255	1.297	0.955 ± 0.011 (1.1%)
SP9 20 kPa with moderator	1.264	1.307	0.956 ± 0.011 (1.1%)

The uncertainties presented in Table 13 for k_1 were derived by repeating the calculations for this correction factor with the effective temperature of the Maxwellian peak changed by 11°C, which is the estimated uncertainty in this quantity. The correction is also sensitive to the value derived for the fraction, $C_{1/E}$, of the sub-cadmium cut-off fluence with a $1/E$ dependence, and on the value chosen for the parameter, μ, which defines the lower limit, $E_{\Delta}=\mu kT$, of the $1/E$ component. However, the uncertainty in k_1 due to the uncertainties in $C_{1/E}$ and μ are negligible compared to those due to the uncertainty in the effective temperature.

Figure 9 illustrates the differences in the spectral distributions, and also shows the shapes of the response functions. The different slopes of the response functions for the bare SP9 counters compared to the response functions for the counters within a moderator explain why the values for k_1 are sometimes greater than 1.0 and sometimes less than 1.0. The response function shape for the 20 kPa SP9 counter in the moderator is almost identical to that for the 200 kPa SP9 counter in the moderator and so is not shown.

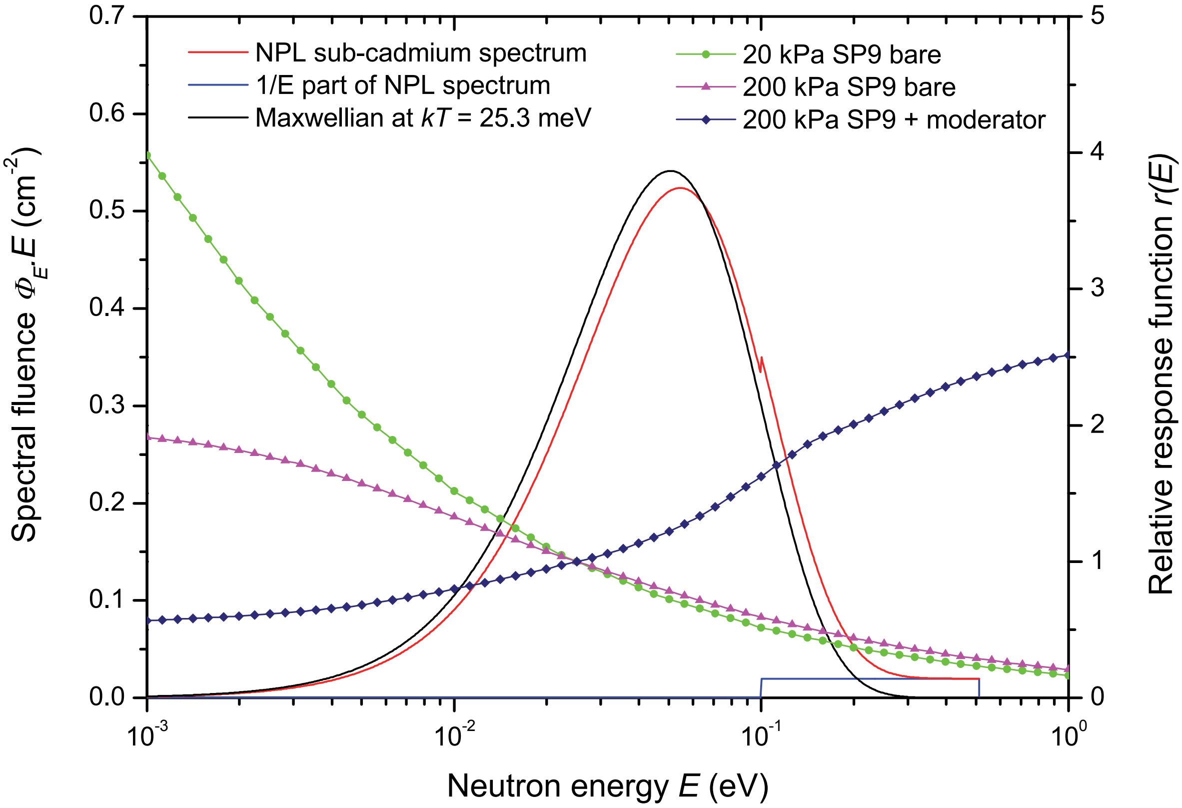

Figure 9. Comparison of the NPL sub-cadmium fluence spectrum with a room-temperature Maxwellian peak. Also illustrated are the response functions used to calculate the correction factors k_1. Note that the response functions have been normalised to unity at 25.3 meV.

5.2 Final results

To obtain the final estimates of the responses in the designated reference field, consisting of a Maxwellian with $kT = 25.3$ meV, the measured responses were multiplied by the relevant k_1 factor from Table 13 to give R_{ref} values.

$$R_{\text{ref}} = k_1 \cdot R_{\text{NPL}} \tag{19}$$

The results are presented in Table 14. Without information from the other participants in the exercise there are only minor comments which can be made about the results. Table 15 compares ratios of R_{NPL} values, for irradiation perpendicular to the beam to those for irradiation parallel to the beam, for the different configurations. The result for the counter perpendicular to the beam is always the larger of the two. For the bare detector this is presumably because of attenuation in the 'top-hat' structure on the opposite side of the spherical counter to the stem (see Fig. 1 in the Appendix to the protocol). For the 200 kPa counter the effect is (8.1 ± 0.5)%, and for the 20 kPa counter it is (6.8 ± 0.4)%. The effect is marginally larger for the 200 kPa counter, possibly because of the presence of ^{3}He in the top-hat structure and the higher gas pressure in this counter. The effect when the counters are enclosed in the polyethylene moderator is much smaller. For the 200 kPa counter the effect is (1.5 ± 0.6)%, and for the 20 kPa counter it is (0.8 ± 0.4)%. The reason for the effect is presumably the same although much reduced because of scatter in the moderating sphere.

Table 14. Final results for the responses of the SP9 counters in the eight different configurations measured. The uncertainties are explained in section 5.3.

Configuration	Response, R_{NPL}, to the NPL sub-cadmium thermal field $n_{th}\overline{v}_{th}$	Response, R_{ref}, in a Maxwellian with $kT = 25.3$ meV
200 kPa SP9 parallel to the beam no polyethylene moderator	2.540 ± 0.062(2.4%)	2.647 ± 0.072(2.7%)
200 kPa SP9 perpendicular to the beam no polyethylene moderator	2.763 ± 0.067(2.4%)	2.879 ± 0.078(2.7%)
20 kPa SP9 parallel to the beam no polyethylene moderator	0.3083 ± 0.0074(2.4%)	0.3246 ± 0.0092(2.8%)
20 kPa SP9 perpendicular to the beam no polyethylene moderator	0.3296 ± 0.0080(2.4%)	0.3471 ± 0.0099(2.8%)
200 kPa SP9 parallel to the beam with polyethylene moderator	1.294 ± 0.031(2.4%)	1.236 ± 0.033(2.7%)
200 kPa SP9 perpendicular to the beam with polyethylene moderator	1.321 ± 0.032(2.5%)	1.261 ± 0.034(2.7%)
20 kPa SP9 parallel to the beam with polyethylene moderator	0.2137 ± 0.0052(2.4%)	0.2043 ± 0.0054(2.7%)
20 kPa SP9 perpendicular to the beam with polyethylene moderator	0.2154 ± 0.0052(2.4%)	0.2059 ± 0.0054(2.7%)

Table 15. Ratios of count rates, R_{NPL} values, for irradiation perpendicular to the beam to those for irradiation parallel to the beam.

Configuration	Ratio of detector response for irradiation perpendicular to the stem and parallel to the stem
200 kPa SP9 bare	1.0808 ± 0.0055(0.51%)
200 kPa SP9 in polyethylene moderator	1.0154 ± 0.0060(0.59%)
20 kPa SP9 bare	1.0682 ± 0.0043(0.40%)
20 kPa SP9 in polyethylene moderator	1.0077 ± 0.0042(0.42%)

One of the reasons for performing measurements with the SP9 detectors bare and within the polyethylene moderator was to obtain information about the mean energy of the neutron distribution. Data for the NPL measurements are given in Table 16. For both the 200 kPa and the 20 kPa detectors the ratio of the bare response to that in the moderator is about 6% higher for the detector perpendicular to the beam than it is for the detector parallel to the beam. This simple reflects the effect of the top-hat structure which reduces the response by about 6% more when the counter is bare than when it is in the moderator – see Table 15.

Table 16. The ratio of a bare SP9 detector response to that of the corresponding counter in the polyethylene moderating sphere for the responses, R_{NPL}, as determined in the NPL thermal column field.

Configuration	Ratio bare detector response to response in moderator sphere
200 kPa SP9 parallel to the beam	1.963 ± 0.013(0.68%)
200 kPa SP9 perpendicular to the beam	2.089 ± 0.030(1.4%)
20 kPa SP9 parallel to the beam	1.4427 ± 0.059(0.41%)
20 kPa SP9 perpendicular to the beam	1.5293 ± 0.063(0.41%)

5.3 Uncertainties

The model equation linking the measured quantities to the final value for the response can be written, c.f. eqs (11) and (19) as:

$$R_{\text{ref}} = k_1 \cdot k_2 \cdot k_3 \cdot R_{\text{NPL}} = k_1 \cdot k_2 \cdot k_3 \cdot \frac{f(N, M_{Ni(i=1\rightarrow 3)}, k^{(\text{Cd})}, N^{(\text{Cd})}, M^{(\text{Cd})}_{Ni(i=1\rightarrow 3)}, M_{\Phi i(i=1\rightarrow 3)})}{\Phi(th)} \quad (20)$$

The term $f(N, M_{Ni(i=1\rightarrow 3)}, k^{(\text{Cd})}, N^{(\text{Cd})}, M^{(\text{Cd})}_{Ni(i=1\rightarrow 3)}, M_{\Phi i(i=1\rightarrow 3)})$ obviously presents a challenge for uncertainty analysis with the contributions to the uncertainties in the input quantities deriving from statistics and dead-time corrections for several measurements at different counting rates. However, these have been combined in the analysis procedure described in section 4.7 to give the uncertainty estimates presented for R_{NPL} in Table 5 to Table 12. Note that the uncertainties in these tables do not include the uncertainty in the fluence *Φ(th)* derived from gold foil measurements during the monitor calibration.

The various k_i values represent corrections to the original measurements all of which are assigned uncertainties although the actual value of k_i may be 1.0. The factor k_1 relates to the correction of the results to what they would have been in a pure Maxwellian spectrum with $kT = 0.0253$ meV, i.e. the factor converting R_{NPL} to R_{ref}. Values are given in Table 13.

A factor k_2 has been included to allow for variations of the fluence per unit monitor reading between the calibration measurement at high demand and the measurements with the SP9 counters, most of which were at a low demand level. As there was no direct evidence of any difference, the value of k_2 was set to 1.0, but with an uncertainty of 1% was applied derived from a review of the stability of the monitors as a function of demand, c.f. section 4.2.

There is evidence from measurements over the years that the calibration of the monitors varies from day to day. Since only one fluence calibration was performed a factor k_3 is included to allow for day to day variations of the monitor calibrations. The standard deviation of monitor calibration values measured over the period from 1999 to 2007, for a height of 1.6 m in the column, is 1.8%. The variations seen over a period of a few days are expected to be smaller than those seen over periods of years. Also, some of the measurements were performed on the same day as the fluence calibration. A value of 1% has therefore been assigned to the uncertainty in k_3 which, as with k_2, is assigned a value of 1.0.

Since the terms in eq. (20) are combined by either multiplication or division the standard uncertainty in the final response can be derived by adding the components for the different terms in quadrature, and the actual values are presented in Table 17. The assumption is made that the various uncertainty components have a normal distribution.

6 CONCLUSIONS

Measurements have been performed of the thermal responses for the two SP9 proportional counters circulated for CCRI key comparison K8. One detector has a gas filling of 200 kPa of ^{3}He and the other 20 kPa. The responses were measured in a number of configurations; specifically with the stem parallel to the NPL thermal column beam and with it perpendicular to the beam, both for the bare detectors and for these detectors in a 7.62 cm diameter polyethylene moderator. Corrections for epi-thermal neutrons were derived from measurements performed using cadmium covers. The final results have been corrected to the values which would be expected in a pure Maxwellian thermal distribution with $kT = 25.3$ meV. For many of the configurations the results with the AIOSAP electronics provided for use in the exercise were found to agree with results obtained using the type of NIM electronics conventionally used with proportional counters at NPL.

Until the results of the comparison exercise are published no conclusions can be drawn about the accuracy of the results. However, the data as presented in Table 14 show some expected features. For example the results for the bare detectors perpendicular to the beam are always higher than the results for the detectors parallel to the beam as expected because of the feature on the opposite side of the spherical SP9 detector to the stem which attenuates the thermal neutron beam. This effect is very much less evident for the detectors in the moderating sphere because of the numerous thermal neutron scattering events within the polyethylene.

The fact that the response of the 200 kPa detector is only about 8.3 times higher than that of the 20 kPa detector, rather than 10 times, is understandable since the 200 kPa detector is sufficiently efficient that response does not increase linearly with pressure in this pressure region.

The fact that the dead-time of the AIOSAP electronics appeared not to be constant with rate was unexpected, and no reason for this has yet been discovered. It is possible that it was a result of the combination of electronic units used with the AIOSAP to provide input to the scaler system. Fortunately, the effect on the final results is not an issue because the vast majority of the measurements were performed at low count rates where the dead-time correction was small. It is, however, an effect which should be investigated when next the equipment is available.

Acknowledgements
The authors would like to thank Andrew Bennett and Sarb Cheema for running the Van de Graaff during the measurements, and Neil Roberts for calculations of neutron attenuation in cadmium covers. The work was funded by the UK National Measurement System Policy Unit of the Department for Innovation, Universities and Skills.

Table 17. Uncertainty components and combined uncertainties. Note all quoted values are standard uncertainties (σ = 1) providing a confidence level of approximately 67% (*k*=1).

Uncertainty component	**Component value**	**Uncertainty**
Counting statistics in beta counting	-	0.2%
Fluence variations during fluence calibration	-	0.1%
Decay effects during gold foil counting	-	0.1%
Dead-time corrections in beta counting	-	0.1%
Reference beta counting efficiency ε_β	~ 0.4	0.3%
Correction to beta counting efficiency for column neutrons *K*	~ 1.05	0.4%
Gold capture cross section, σ_0	98.69 b	0.2%
Thermal self-shielding factor G_t	0.9843	0.3%
Departure of gold cross section from 1/*v* dependence *g*	1.0046	0.1%
Cadmium attenuation correction *F*	1.01	0.1%
Maxwellian effective temperature *T*	22.6°C	0.3%
Foil mass	~ 96 mg	0.1%
Height of gold foil and of SP9 detectors	1.6 m	0.3%
Combined uncertainty in the Westcott fluence $n_{th}v_0$		**0.8%**
Effect of uncertainty in T on going from $n_{th}v_0$ to $n_{th}\overline{v}_{th}$	-	1.7%
Relative intensity of epithermal component *r*	~ 0.02	0.1%
Uncertainty in Westcott cut-off parameter μ	3.681	0.2%
Combined uncertainty in the true fluence $n_{th}\overline{v}_{th}$		**1.9%**
Variation of the fluence with demand k_2	1.0	1.0%
Variation of monitor calibration with time (days) k_3	1.0	1.0%
Combined uncertainty in the response values R_{NPL}*		**2.4%**
Correction to results in a pure Maxwellian spectrum k_1	0.955 - 1053	1.1% - 1.5%
Combined uncertainty in the response values R_{ref} *		**2.6% - 2.8%**

* Note: these uncertainties exclude counting statistics and dead-time for the SP9 counter and monitors, and the uncertainty in $k^{(\mathrm{Cd})}$. These differ for each measured response, varying from 0.2% to 0.5%.

REFERENCES

1 C.H. Westcott, W.H. Walker, and T.K. Alexander, *Effective cross sections and cadmium ratios for the neutron spectra of thermal reactors,* Proceedings of the Second United Nations international conference on the peaceful uses of atomic energy, Vol. 16 Nuclear data and reactor theory, (UN, Geneva, 1958).

2 E.J. Axton, *Absolute measurement of the neutron flux density in the A.E.R.E reactor GLEEP,* J. of Nucl. Energy Parts A/B 17, 125-135, 1963.

3 S.J. Boot, *Calibration of reference thermal and epithermal neutron flux densities from the GLEEP reactor at AERE Harwell,* Nucl. Inst. and Meths. 164, 513-519, 1979.

4 D.J. Thomas and N. Soochak, *Determination of the ^{3}He number density for the proportional counter used in the NPL Bonner sphere system,* NPL Report RS(EXT)104, (NPL, Teddington, July 1988).

5 T.B. Ryves and E.B. Paul, *The Construction and Calibration of a Standard Thermal Neutron Flux Facility at the National Physical Laboratory*, J. Nucl. Energ. 22(12), 759-775, 1968.

6 A.D. Carlson, W.P. Poenitz, G.M. Hale, R.W. Peelle, D.C. Dodder, C.Y. Fu, and W. Mannhart, *The ENDF/B-VI Neutron Cross Section Measurement Standards,* NIST Report NISTIR 5177, National Institute of Standards and Technology, Gaithersburg, MD, USA, 1993.

7 P. Kolkowski and D.J. Thomas, Measurement of the fast neutron component in the beam of the NPL thermal neutron column using a Bonner sphere spectrometer, NPL Report CIRM 28, (NPL, Teddington, May 1999).

8 K.W. Geiger and L. van der Zwan, *Slowing Down Spectrum and Neutron Temperature in a Thermal Neutron Flux Density Standard,* Metrologia, 2, 1-5, 1966.

9 David J. Thomas and Peter Kolkowski, *Thermal fluence and dose equivalent standards at NPL,* NPL Report DQL RN008, March 2005

10 N.J. Roberts, NPL, private communication.

11 D.J. Thomas and N. Soochak, *Determination of the ^{3}He number density for the proportional counter used in the NPL Bonner sphere system*, NPL Report RS(EXT)104, July 1988.

12 http://www.nag.co.uk/

Appendix A: Protocol

CCRI(III)-K8: Key Comparison for Thermal Neutron Fluence Measurements

Comparison Protocol

Introduction

Reference facilities for the fluence of thermal neutrons have been constructed in several ways. Designs based on thermal columns or neutron guides at fission reactors and moderation of fast neutrons produced by accelerators or radionuclide sources have been employed. The details of the phase space density of neutrons at such facilities may differ significantly. In particular, the angular distribution may vary from almost isotropic to unidirectional. Furthermore, the spectral distribution can deviate from a Maxwellian or correspond to a temperature different from that of the moderator. Also the contamination of the thermal beam or field with epithermal neutrons above the cadmium threshold is related to details of the construction of the facility.

To reveal differences in the characteristics of the facilities participating in a comparison of thermal fluence measurements, a transfer instrument, or combination of instruments, is required that is sensitive to the actual spectral distribution. Therefore a comparison is proposed which uses transfer instruments with opposite energy dependency of their response, i.e. one or more instruments for which the response decreases with neutron energy and one or more instruments with increasing response over the thermal region. Basically, the ratio of the responses of two such instruments can be used as an indicator to assess the temperature parameter kT of the spectral distribution.

Transfer Instruments and Ancillary Equipment

The pilot laboratory will provide two spherical proportional counters filled with ^{3}He as transfer instruments.

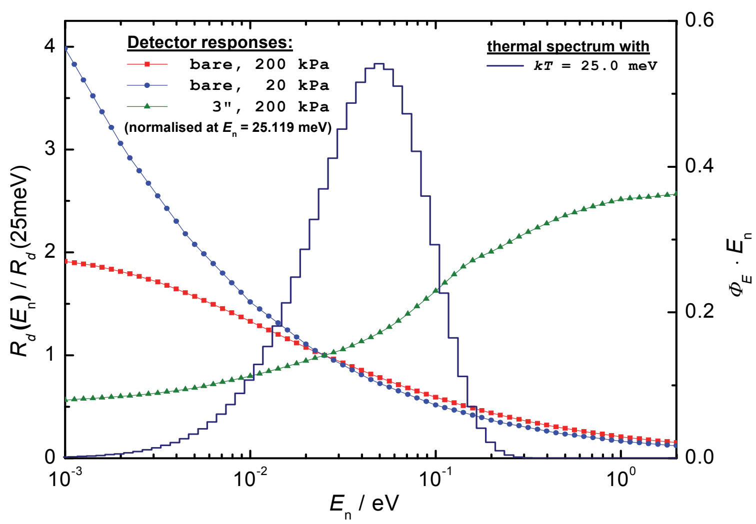

Fig. 1 Relative response $r(E) = R(E)/R(E_{ref})$ for the three transfer instruments as calculated with MCNP (left axis) for $E_{ref} = 25.119$ meV. Also shown is the relative Maxwellian spectral fluence distribution for $kT = 25$ meV (right axis). The responses for the bare counters and the counter in moderator sphere were calculated using MCNP for a parallel beam incident perpendicular and parallel to the symmetry axis, respectively.

The counters are of the CENTRONIC SP9 type and have nominal ^{3}He pressures of 20 kPa and 200 kPa, respectively. In addition, a spherical polyethylene (PE) moderator, 7.62 cm (3") in diameter, is provided to modify the energy dependence of the response of the 200 kPa counter. Therefore three transfer devices are available for the comparison exercise. The selection of the most appropriate bare counter will be made by the participant based on count rate considerations. If possible, all three instruments should be used. The participants are also encouraged to use the 20 kPa counter with the PE moderator if the count rate is sufficient.

The relative response $r(E) = R(E)/R(E_{ref})$ for $E_{ref} = 25.3$ meV, as calculated using MCNP [1], is shown in Fig. 1 for the two bare counters and the 200 kPa counter in the 3" PE moderator. The responses $R(E_{ref})$ for the bare 200 kPa counter, the bare 20 kPa counter and the 200 kPa counter in the 3" PE moderator sphere are about 3 cm^2, 0.4 cm^2 and 1 cm^2, respectively (these numbers are meant for count rate estimates only and can deviate from the result of a Monte Carlo calculation for the actual parameters of the counters by up to 20%!). The relative response of the 20 kPa counter in the moderator sphere has still to be calculated and will be provided by the pilot laboratory at a later time.

The signals provided by the counters are processed by an electronic module (AIOSAP) [2] which comprises a high-voltage supply, a pre-amplifier, a shaping amplifier and two discriminators. This module is also provided by the pilot laboratory. One discriminator (D1) is used to separate events resulting from the ^{3}He(n,p)^{3}H reaction from those due to photons and electronic noise. The number N of the TTL output pulses of D1 have to be counted by the participant to determine the response R in his neutron field or beam. For this purpose, a counting module has to be provided by the participant. The proper setting of D1 has to be checked individually using a Multichannel Analyser (MCA) provided by the participant. The dead time τ introduced by D1 was measured using the pulse interval method. The effective dead time resulting from the interval distribution shown in Fig. 2 is $\tau = (7.2 \pm 0.9)$ µs. The interval distribution is in compliance with the assumption of a non-extending dead time. More details on the mounting and operation of the detectors and the AIOSAP module can be found in the appendix.

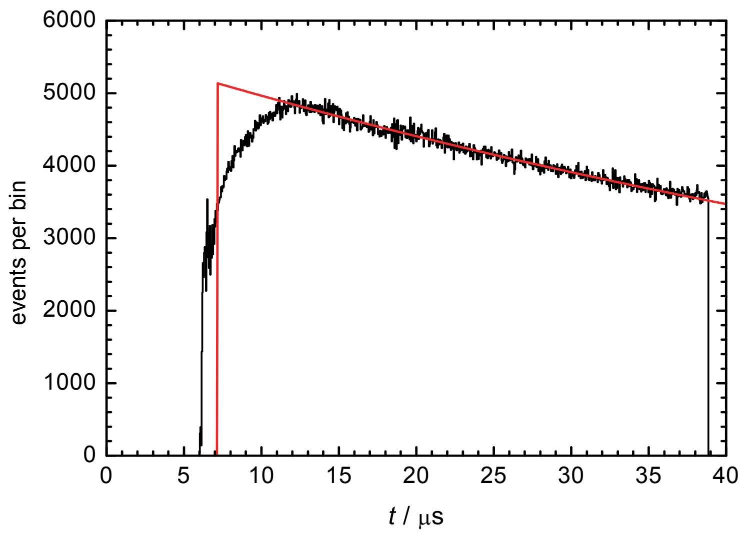

Fig. 2 Distribution of the time intervals between successive output pulses of the discriminator D1 (black histogram). The red solid line shows the fitted interval distribution $N(t) = N_0 \cdot \exp(-\rho(t-\tau_{eff}))$ with an effective non-extending dead time $\tau_{eff} = (7.2 \pm 0.9)$ µs.

Two tight-fitting cylindrical cadmium shields 1 mm in thickness are provided for measuring the effect of epithermal neutrons above the cadmium threshold on the bare counters and the 200 kPa counter inside the 3" PE moderator, respectively.

Determination of the Response

The participants shall determine the response R_{ref} of the counters for a homogeneous unidirectional irradiation with neutrons with a Maxwellian fluence distribution $\Phi_E^{(\mathrm{ref})}$ characterised by a temperature parameter $kT = 25.3$ meV.

$$\frac{\Phi_E^{(\mathrm{ref})}\,\mathrm{d}E}{\Phi^{(\mathrm{ref})}} = \left(\frac{E}{kT}\right)\exp\left(-\frac{E}{kT}\right)\frac{\mathrm{d}E}{kT}$$

This requires that the relative spectral fluence (Φ_E/Φ) and the fluence Φ below the nominal cadmium threshold at 0.68 eV is determined in the neutron field or beam at the same location and under the same conditions as for the measurement with the counter. An appropriate monitoring system may be necessary to relate these two measurements if they cannot be carried out simultaneously. Dead time losses shall be kept below 10% by selecting the most appropriate counter and adjusting the fluence rate, if possible.

Appropriate correction factors have to be determined if the actual irradiation conditions deviate from the reference conditions. Most important, the spectral distribution of the actual neutron field can deviate from a Maxwellian with the reference temperature parameter. The relative responses shown in Fig. 1 are provided in numerical form for the calculation of correction factors. The correction factor k_1 for the spectral distribution is given by

$$k_1 = \frac{\int_0^{\infty}\left(\Phi_E^{(\mathrm{ref})}/\Phi^{(\mathrm{ref})}\right) r(E)\,\mathrm{d}E}{\int_0^{E_{\mathrm{Cd}}}\left(\Phi_E/\Phi\right) r(E)\,\mathrm{d}E}$$

where the integration over the relative spectral fluence (Φ_E/Φ) of the neutron field or beam is extended up to the nominal cadmium threshold energy E_{Cd} at 0.68 eV [3]. Also dead time losses have to be corrected for. The dead time correction k_2 is

$$k_2 = \frac{1}{1-\tau\left(\mathrm{d}N/\mathrm{d}t\right)}$$

for a non-extending dead time.

Other correction factors can arise, for example, from the inhomogeneous fluence distribution over the sensitive area of the counter. This effect can either be corrected experimentally by using a scanning procedure or calculated using the Monte Carlo method. Also the angular distribution of the spectral fluence may require corrections if fields are used which are not unidirectional. An MCNP model of the detector for the calculation of correction factors can be made available by the pilot laboratory on request. Correction factors are also required if the fluence is not measured at the same position as the counter or, in case of inhomogeneous fields, the sensitive area of the instrument used for the fluence measurement is different from that of the counter.

With these correction factors k_i and the number of monitor counts M_Φ , M_N and $M_N^{(\mathrm{Cd})}$ for the measurement with the instrument used for the fluence measurement, the counter without cadmium cover and with cadmium cover, the response is given by

$$R_{\text{ref}} = \prod_{i=1}^{n} k_i \cdot \frac{\left(N / M_N - k^{(\text{Cd})} N^{(\text{Cd})} / M_N^{(\text{Cd})}\right)}{\left(\Phi / M_\Phi\right)}$$

Here $n \geq 2$ denotes the number of correction factors k_i. The correction factor $k^{(\text{Cd})}$ accounts for the absorption of epithermal neutrons in the Cd shield (1 mm Cd + 1 mm Al) and has to be calculated by the participants if this correction cannot be neglected.

Report

The report to be delivered for the evaluation of the results has to include the following details:

- A brief description of the calibration facility and the methods used for characterising the neutron field or beam.
- Specification of the spectral neutron fluence (Φ_E/Φ) and the total fluence Φ (below the nominal cadmium threshold at 0.68 eV) and a documentation of the traceability to primary national standards.
- Description of the measurements carried out with the transfer instruments including readings N and $N^{(\text{Cd})}$ of the transfer instruments in the neutron fields or beams, monitors readings M and $M^{(\text{Cd})}$, measurement times and pulse-height spectra of the detectors measured in coincidence with the discriminator signal.
- Evaluation of the response R_{ref} under reference conditions including the values of all corrections factors k_i as well as a description of how these values were calculated.
- Evaluation of an uncertainty budget for R_{ref}. All uncertainties have to be specified as standard measurement uncertainties for a coverage factor $k = 1$. The recommendations of the *Guide to the Expression of Uncertainty in Measurement* [4] should be followed.

Evaluation and Publication of the Results

The results reported by the participants will be evaluated by the pilot laboratory. The key comparison reference values (KCRV) [5] will be calculated for each of the three transfer instruments as the weighted mean of the results reported by the participants. Reciprocals of the uncertainties reported by the participants will be used to calculate the weights. From the KCRV and the specified uncertainties, the degree of equivalence (DoE) will be calculated. After discussion and approval of the evaluation report by all participants, the results of the comparison will be published on part C of the Key Comparison Data Base of the BIPM (type B final report) and in Metrologia (short summary and results).

Because the pilot laboratory will also participate in the comparison exercise, all reports will have to be filed at the BIPM. The BIPM will forward the reports to the pilot laboratory after the pilot laboratory has filed its report.

Transport Arrangements

The pilot laboratory will perform a stability test with the two counters after each return from a participant. In case of any changes, the last participant will be notified and appropriate action will be taken. The pilot laboratory will cover the expenses for shipping the equipment to the participants while the participants have to cover the cost of the return shipments.

Time Table

Laboratory	**Date of receipt**	**Date of return**
AIST	Nov. 2006	Jan. 2007
NPL	Feb. 2007	Apr. 2007
CIAE	May 2007	Jul. 2007
PTB (pilot lab.)	Nov. 2007	Jan. 2008
NIST	Mar. 2008	May 2008
IRSN	Nov. 2008	Jan. 2009

The indicated dates refer to the beginning of a month

References

[1] X-5 Monte Carlo Team, *MCNP – A General Monte Carlo N-Particle Transport Code, Version 5*, Report LA-UR-03-1987, Los Alamos National Laboratory, April 24, 2003

[2] A.V. Alevra, *All-in-one Spectrometry Analogue Processor AIOSAP-01, Manual*, Braunschweig 2006

[3] K.H. Beckurtz and K. Wirtz, *Neutron Physics*, paragraph 12.2.2., Springer-Verlag Berlin, Göttingen, Heidelberg, New York, 1964

[4] *Guide to the Expression of Uncertainty in Measurement*. International Organisation for Standardisation, Geneva, Switzerland, 1995. ISBN 92-67-10188-9, Second Edition

[5] M.G. Cox, *The Evaluation of Key Comparison Data: An Introduction*, Metrologia **39** (2002) 587-588 and
M.G. Cox, *The Evaluation of Key Comparison Data*, Metrologia **39** (2002) 589-595

Appendix: Instruction for use of the equipment provided by the pilot laboratory

General Remarks

Two spherical ^{3}He detectors of the CENTRONIC SP9 type were chosen for the key comparison for thermal neutron fluence measurements. The two bare detectors have nominal ^{3}He pressures of 200 kPa (SP9/20) and 20 kPa (SP9/200). To modify the fluence response of the two detectors a spherical polyethylene (PE) moderator 7.62 cm (3″) in diameter is provided. For the determination of the fluence of epithermal neutrons, two cadmium shields are provided, one for the bare counter and one for the counter inside the moderator. The thickness of the cadmium layer is 1 mm. An electronic module (AIOSAP) is provided which comprises a high voltage supply and the analogue pulse processing and discrimination units. The participants have only to set the appropriate pulse-height threshold and count the number of events above this threshold using a counting module for standard TTL pulses.

Operation of the ^{3}He Proportional Counters

The bare counter and the high-voltage cable connecting the counter to the AIOSAP module are shown in Fig. 1. As can be seen from this figure, the bare SP9 has a nose and a stem with a special (PET) socket (15) on the opposite side of the spherical sensitive volume. The serial numbers of the SP9/20 and the SP9/200 counters are 9313-111 and 8916-104, respectively. They are indicated on the stem together with the nominal pressure and the appropriate voltage.

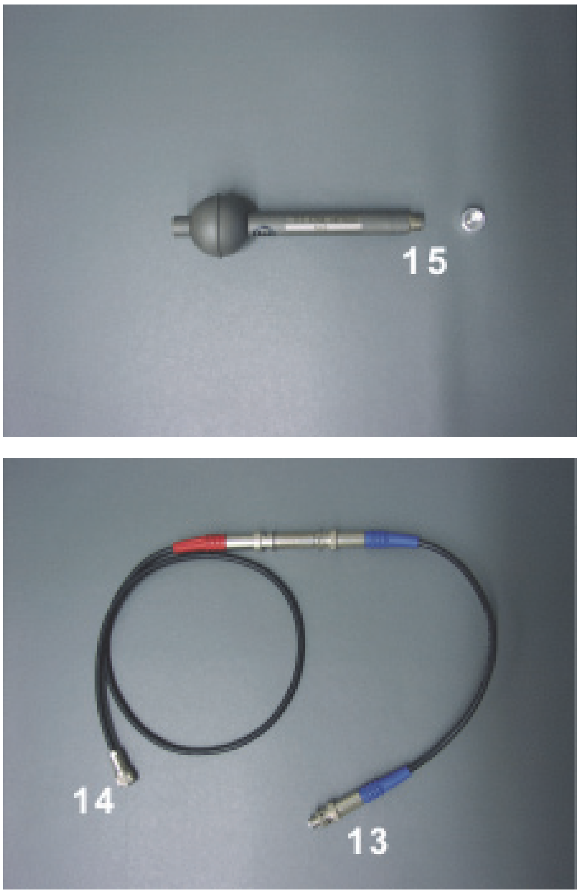

Fig. 1 SP9 counter (upper panel) and the high-voltage cable connecting the counter to the AIOSAP module (lower panel)

A short cable interfacing this special socket to a standard SHV socket is provided. The high-voltage cable connecting the detector with the AIOSAP module should be as short as possible for optimal pulse processing.
Fig. 2 shows the mounting of the bare counter in the cadmium shield. The counter is connected to the socket on the inner side of the lid and then inserted into the cylindrical shield. The shield for the bare counter has a ring at the bottom with accepts the nose of the counter and fixes its position.
The sequence of steps for assembling the moderator sphere with the counter inside and for inserting the sphere in its cadmium shield is shown in Fig. 3. The diameter of the cylindrical shield for the counter inside the spherical moderator is only slightly larger than the diameter of the moderator sphere. This defines the position of the counter inside the shield. When mounting the detectors inside the shields, any excessive force has to be avoided to prevent damage to the counters! The outer dimensions of the shields are shown in Fig. 4.

For the bare counter, the point of reference is marked by the rims of the spherical sensitive volumes. The positions of points of reference of the counters inside the shields are marked on the outside of the shields.

For the bare counter, the symmetry axis must be oriented perpendicular to the neutron beam direction. If the counter is operated inside the moderator, the beam direction must be parallel to the symmetry axis of the counter with the beam incident on the nose. The same applies for the measurements with the cadmium shields.

Operation of the AIOSAP module

The front panel of the AIOSAP module is shown in Fig. 5. A detailed manual is provided with the module. If necessary, the unit can be operated with the internal set of batteries instead of using the external power supply shown in Fig. 6. The settings when not in operation are indicated in Table 1. The controls secured by the red plastic caps should not be changed by the participants.

Table 1 Settings for the AIOSAP module when not in operation. The labels refer to Fig. 5.

1. Switch (1) ITG : OFF
2. Switch (2) Shaping : 1µs
3. Switch (3) Power : OFF
4. Switch (4) HV: OFF
5. Switch (5) COARSE GAIN: x2
6. Switch (6) Pulser: P
7. Switch (7) Display: HV
8. High-voltage control (8): 0

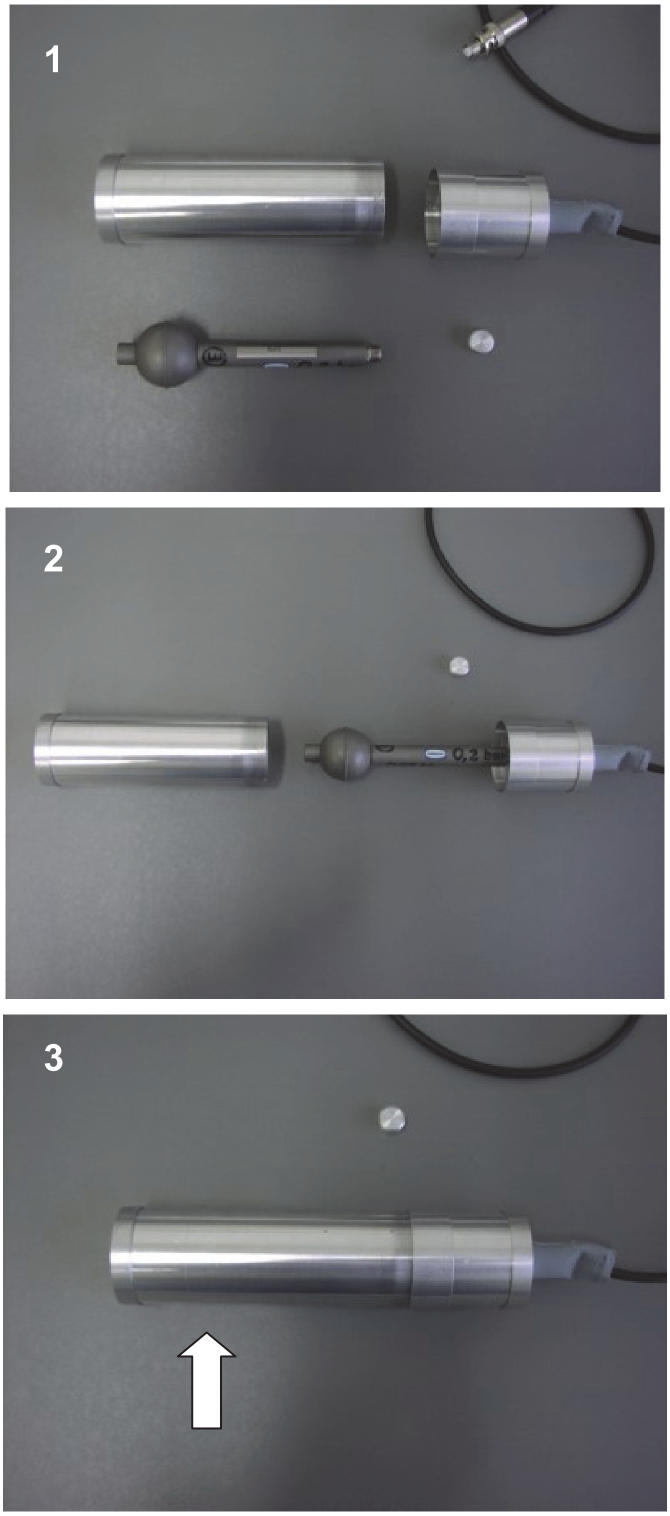

Fig. 2 Insertion of the bare counter into the cadmium shield. The beam has to be incident perpendicular to the stem of the counter.

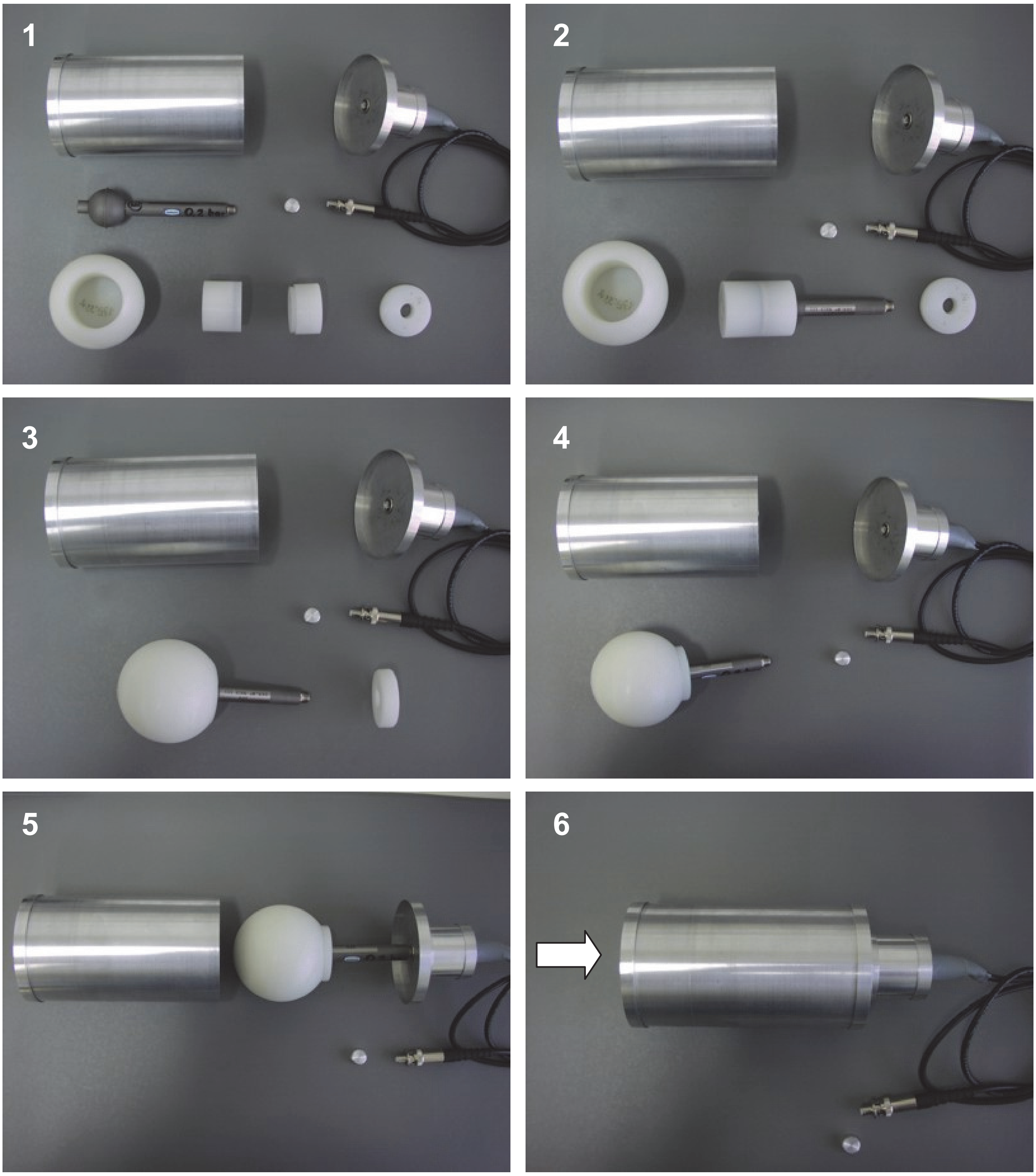

Fig. 3 Mounting of the moderator sphere with the counter inside and insertion into the cylindrical cadmium shield. The beam has to be incident parallel to the detector stem.

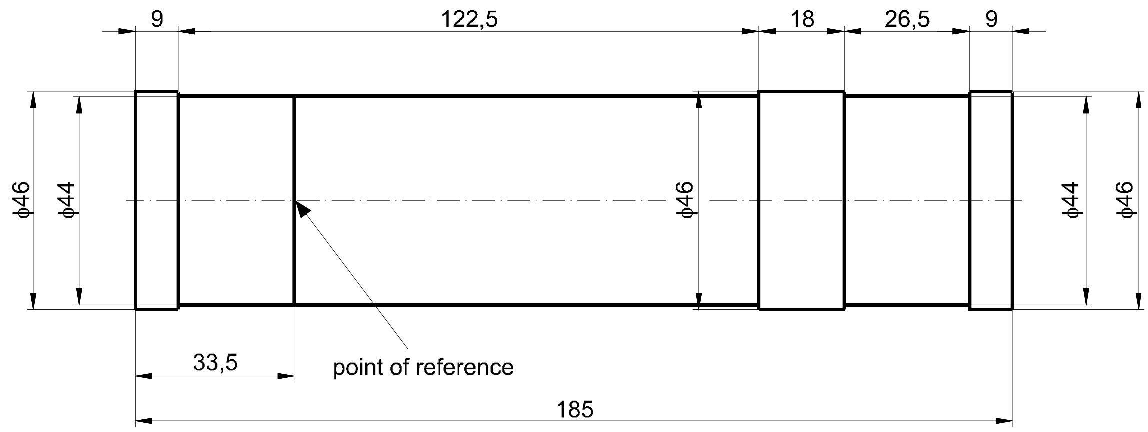

shield for bare SP 9 counter

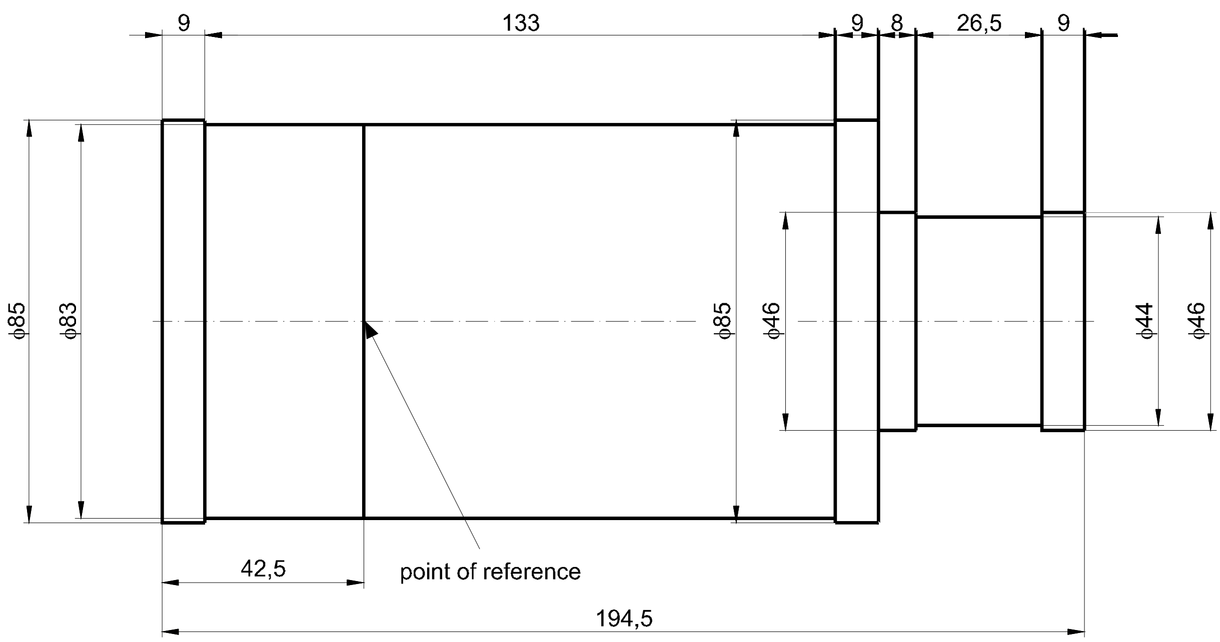

shield for 3" sphere with SP 9 counter

Fig. 4 Outer dimensions of the shields for the bare SP9 counter and the 3" moderator sphere. The walls of the shields consist of 1 mm AlMg3 on the outside and an inner layer of 1 mm cadmium. The point of reference is on the axis of the cylinders at the distances from the end caps indicated on the drawing. These positions are marked by lines engraved in the housings.

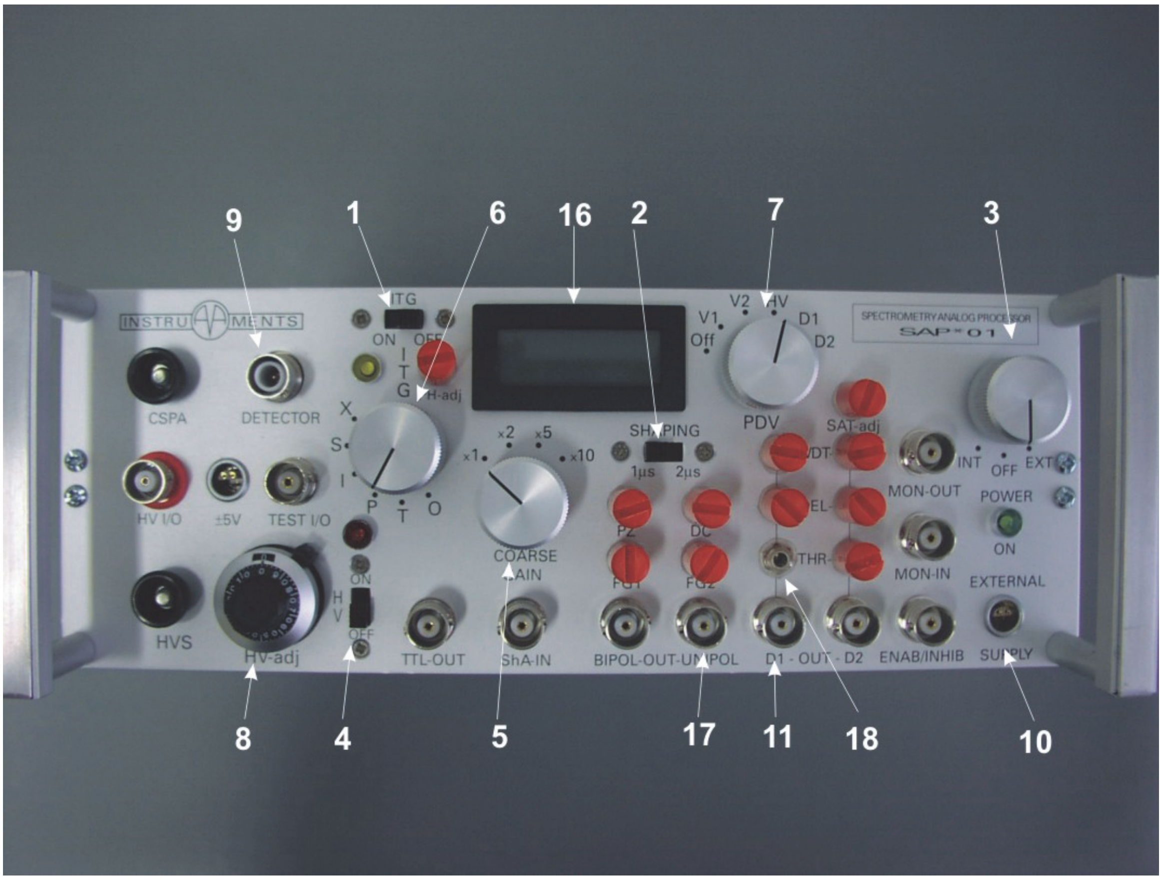

Fig. 5 Front panel of the AIOSAP module. The labels of the controls, displays and connectors are explained in the text and Table 1.

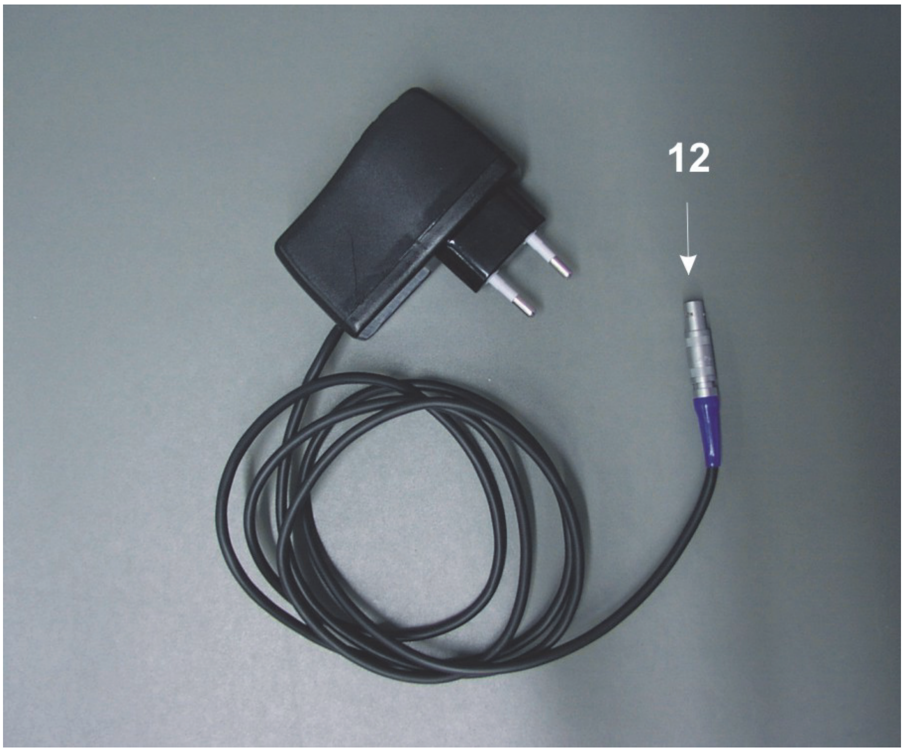

Fig. 6 External power supply for the AIOSAP module. The power supply operates on 110 V - 230 V AC. The switch on the power supply has to be set to 6 V.

The start-up procedure for the AIOSAP module is as follows:

1. Connect plug (12) of external power supply to socket (10).
2. Connect plug (13) of high-voltage cable to socket (9).
3. Connect plug (14) of high-voltage cable to socket (15).
4. Connect discriminator out (11) to the counting module supplied by the participant by a 50 Ω BNC cable.
5. Set switch (3) to EXT.
6. Set switch (4) to ON.
7. Set the high-voltage control (8) slowly to the appropriate value. The voltage applied to the counter is shown on the display (16).
   Counter SP9/200: 795 V
   Counter SP9/20: 755 V

Reminder: set the voltage control (8) to zero before connecting or disconnecting a counter!

The discriminator D1 is used to separate events induced by photons or electronic noise from events caused by ^{3}He(n,p)^{3}H reactions. The discriminator output signal from the BNC socket (11) is fed to a counting module which has to be supplied by the participant. The TTL pulses from the discriminator D1 have an amplitude of 5 V and a duration of 6 μs (see Fig. 7). The dead time introduced by the discriminator was measured to be (7.2±0.9) μs.

To check the proper setting of the discriminator, a pulse-height spectrum has to be measured. For this purpose, the unipolar signal available at BNC socket (17) should be used. The data acquisition system has to be provided by the participant. It has to be triggered or operated in coincidence mode using the discriminator signal available at BNC socket (11). The width of this signal is adjusted to 6 μs (see Fig. 7). The discriminator threshold was set to about 15% of the pulse height of the main peak (see Fig. 8) to effectively discriminate against electronic noise and photon-induced events. The setting of the discriminator D1can be changed by the participant using potentiometer (18) if this turns out to be necessary.

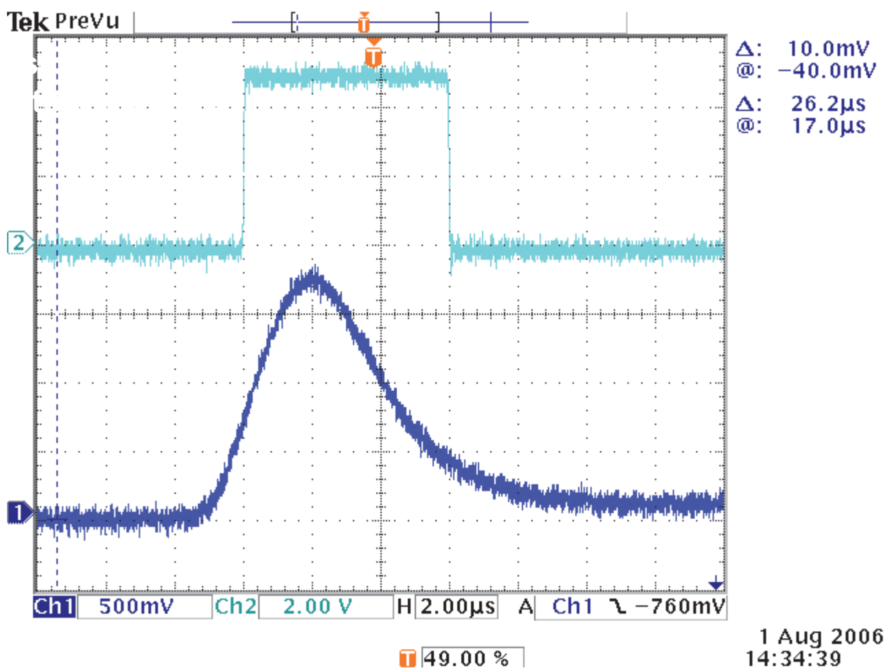

Fig. 7 Timing diagram of the unipolar analogue signal (lower trace) and the TTL discriminator signal (upper trace)

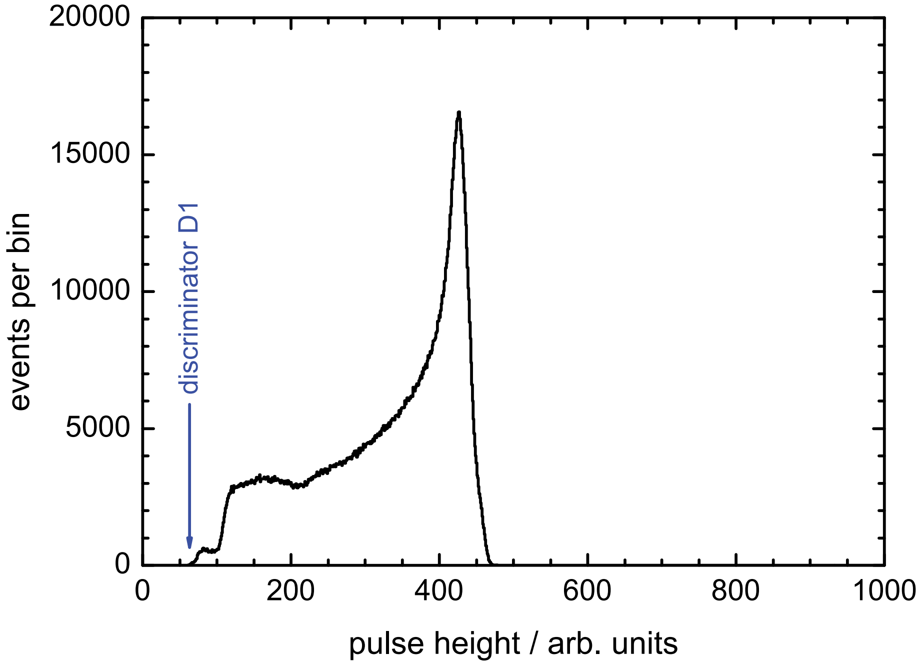

Fig. 8 Pulse-height spectrum of the bare SP9/200 counter measured using a thermal neutron field.

Measurements with the cadmium shield showed that the additional photon background resulting from neutron capture in the cadmium is negligible and shows up only at in the pulse-height region below the threshold.

Appendix B: Printout of Westcott fluence analysis

Output from the Fortran program, Westcott, which is used to calculate the fluences from the gold foil saturated disintegration rates

```
PROGRAM WESTCOTT  -  Version 1.2 compiled    June 2005
THERMAL AND EPITHERMAL FLUENCES CALCULATED FROM FOIL ACTIVATION

Run date: 13-02-2009                Run time: 18:26:29

Au 109 bare + Au 900 in Cd, NPL col 1.6m posn. Evac. Small foils.

  D0(bare)     D0(Cd)    Eff Temp K    FC rate
 5.0537E+00  6.3350E-01  3.1510E+02  4.5792E+03


     FCd      At Wt        G(th)      W-cott g    Sigma(0)
 1.0100E+00  1.9697E+02  9.8430E-01  1.0046E+00  9.8690E+01


   G(res)       S(0)     Res Attn f        W       W-cott K       mu
 3.6700E-01  1.7300E+01  9.9000E-01  2.7000E-02  1.9939E+00  3.6810E+00


 CALCULATED RATIOS AND FLUENCES  (kT = 0.0272 eV)

    R(Cd)      r(T/T0)        r        R(1/v)
 7.9774E+00  2.0715E-02  1.9996E-02  9.6253E+01


  n(th)v(0)     nv(0)     n(M)v(0)   n(1/E)v(0)    n(1/E)/n(M)
 1.4794E+04  1.4949E+04  1.4597E+04  3.5160E+02    2.4087E-02


  For the KT and mu values used:
  E(Cd) =  5.1227E-01   El =   9.9949E-02
  epithermal fraction [4*r/sqrt(Pi*mu)] =   2.3520E-02

  For the Maxwellian distn. v(bar)/v(0) =   1.1690E+00
  n(M)v(bar) =   1.7064E+04
  n(1/E)v(bar) per unit lethargy =   3.4942E+02
  n(1/E)v(bar) between El and E(Cd) =   5.7102E+02
  ( 3.346 % of n(M)v(bar)  3.238 % of n(th)v(bar))

  For sub-Cd neutrons:
  n(th)v(bar) =   1.7635E+04
  v(bar)/v(0) =   1.1921E+00

  For the epi. fluence El to E(Cd) v(bar)/v(0) =   2.9090E+00
  and thus v(bar) for this region =   6.3998E+05 cm/sec
  n(M)  =   6.6351E-02
  n(th) =   6.7244E-02
  n(1/E) between El and E(Cd) =   8.9225E-04
  ( 1.345 % of n(M)  1.327 % of n(th))


  Fluences divided by the fission chamber count rate

  n(th)v(0)     nv(0)     n(M)v(0)   n(th)v(bar)   n(M)v(bar)
 3.2306E+00  3.2645E+00  3.1877E+00  3.8511E+00  3.7264E+00
```